Identification and characterization of thousands of bacteriophage satellites across bacteria

Jorge A Moura de Sousa, Alfred Fillol-Salom, José Penadés, Eduardo P.C. Rocha

Nucleic Acids Research, 2023 **1**
https://doi.org/10.1093/nar/gkad123

Identification and characterization of thousands of bacteriophage satellites across bacteria

Jorge A. Moura de Sousa [1,*], Alfred Fillol-Salom[2], José R. Penadés [2] and Eduardo P.C. Rocha [1,*]

[1]Institut Pasteur, Université Paris Cité, CNRS, UMR3525, Microbial Evolutionary Genomics, Paris 75015, France and [2]Center for Bacterial Resistance Biology, Imperial College London, London, SW7 2AZ, UK

Received September 19, 2022; Revised January 19, 2023; Editorial Decision February 08, 2023; Accepted February 10, 2023

ABSTRACT

Bacteriophage–bacteria interactions are affected by phage satellites, elements that exploit phages for transfer between bacteria. Satellites can encode defense systems, antibiotic resistance genes, and virulence factors, but their number and diversity are unknown. We developed SatelliteFinder to identify satellites in bacterial genomes, detecting the four best described families: P4-like, phage inducible chromosomal islands (PICI), capsid-forming PICI, and PICI-like elements (PLE). We vastly expanded the number of described elements to ∼5000, finding bacterial genomes with up to three different families of satellites. Most satellites were found in Proteobacteria and Firmicutes, but some are in novel taxa such as Actinobacteria. We characterized the gene repertoires of satellites, which are variable in size and composition, and their genomic organization, which is very conserved. Phylogenies of core genes in PICI and cfPICI indicate independent evolution of their hijacking modules. There are few other homologous core genes between other families of satellites, and even fewer homologous to phages. Hence, phage satellites are ancient, diverse, and probably evolved multiple times independently. Given the many bacteria infected by phages that still lack known satellites, and the recent proposals for novel families, we speculate that we are at the beginning of the discovery of massive numbers and types of satellites.

INTRODUCTION

Bacteriophages (phages) shape the evolution and composition of bacterial communities, both through predation and by driving horizontal gene transfer between bacterial cells (1,2). Phages are notorious parasites of bacteria and are themselves parasitized by phage satellites. These elements lack some of the functions required for autonomous horizontal transfer, which they hijack from helper phages. In the past, phage satellites were sometimes mistaken for defective phages, even if their gene repertoires rarely have genes in common with phages. Yet, some phage satellites do have phage-like genes. For example, the phage-inducible chromosomal islands (PICI) of *Staphylococcus aureus* typically encode packaging functions homologous to those of the helper phage 80α (3,4). In contrast, the P4 satellite of *Escherichia coli* has few homologs with its P2 helper phage (5). Phage satellites exploit their helper phages through molecular mechanisms that depend on the type of satellite. The extent of this exploitation is variable, as are its consequences for phage reproduction. Phage-inducible chromosomal island-like elements (PLE) of *Vibrio cholerae* completely block the propagation of the helper lytic phage ICP1 (6) and PICI can severely reduce phage reproduction (7). On the other hand, the recently identified capsid-forming PICI (cfPICI) EcCIEDL933 of *E. coli* has negligible effects on phage fitness (8). Beyond their effect on phage infection, satellites provide their bacterial hosts with accessory potentially adaptive functions. For example, some PICI encode virulence factors, like toxins, or antibiotic resistance genes (3), and some P4-like elements and PICI encode anti-phage immunity systems (9,10). Hence, satellites have wide functional and ecological impacts in phages and in bacteria.

The few satellites that have been studied in detail encode a set of core functions that are sometimes non-homologous but can be grouped into four major groups: integration, regulation, replication and hijacking. All known satellites are integrated in chromosomes, which usually occurs by the action of an integrase of the Tyrosine recombinase family. Upon excision, satellites require specific replicases to replicate before being packaged in viral particles. Genetic regulation is essential for the success of the element. On one hand, the element may remain for long periods of time largely silent in the chromosome before entering in contact with an infecting helper phage. On the other hand, upon co-infection by a helper phage, the satellite must coordinate its expression with the latter. One of the most fascinating

*To whom correspondence should be addressed. Tel: +33 1 45 68 89 83; Email: jorge-andre.sousa@pasteur.fr
Correspondence may also be addressed to Eduardo P.C. Rocha. Email: erocha@pasteur.fr

traits of satellites is the diversity of mechanisms they use to subvert the host phage viral particles. Some phage satellites physically constrain the size of the viral capsid produced by the phage, so that phage DNA does not fit inside—but the satellite DNA does (11). Other satellites directly redirect the packaging of their own DNA into the viral capsid by encoding sequences that mimic the phages' terminases (12).

Phage satellites have only recently emerged as a distinct class of mobile elements. Even if the satellite P4 was discovered decades ago, few phage satellites have been detected in genomes until very recently. Some of these mobile elements were either mistaken as plasmids (13) or annotated as defective phages or prophage-like remains (14). However, this perspective has recently changed. There is increasing evidence of the pervasiveness and importance of phage satellites (15,16), and recent work has started to uncover the diversity of these elements, especially within a given family (5,12). These studies have helped recognize phage satellites as characteristic mobile elements that have specialized in being mobilized by fully functional phages. Moreover, there have been recent reports of genomic islands transduced by phages that are different from known phage satellites, which suggests that different types of satellites remain to be discovered (17,18).

Many studies have unraveled the mechanisms of function of the model satellites for each of the known families, as well as their importance in bacterial evolution and pathogenicity (4,9,10,19). But their abundance in genomes is poorly studied for lack of a systematic way to identify them. This is important, because the small number of known phage satellites has limited their comprehensive study in terms of evolution and diversity. Recently, we have reported the discovery of ca. 1000 elements of the P4-like family, which has led to novel insights regarding their diversity, evolution, genomic composition and organization (5). Here, we systematize and expand this analysis to all currently known phage satellite families and report the discovery of ca. 5000 putative phage satellites in complete bacterial genomes. This allowed us to study the abundance of phage satellites within and across bacterial hosts, and to understand how the different families of satellites are organized in terms of their core components and genetic repertoires. We also sought to understand whether there are similarities between the different main families of phage satellites, and whether there are different sub-families within them. Our approach allows for a novel, automatic detection of phage satellites, of all best-known families, in bacterial genomes and sheds light on the abundance and diversity of these mobile elements.

MATERIALS AND METHODS

Genomic datasets

We retrieved all the complete genomes of the NCBI non-redundant RefSeq database (ftp://ftp.ncbi.nlm.nih.gov/genomes/refseq/, last accessed in March 2021), including 21 084 bacteria, 21 520 plasmids and 3725 phages. The distribution of the bacterial genomes in phylum, class and order are shown in File S1. Additional phage nucleotide sequences, corresponding to all complete or draft genomes, were obtained from the NCBI database (accessed in May 2021). We made a quality filter to retain only those sequences with 10 predicted proteins, resulting in a dataset of 15 558 phages. We also retrieved and annotated both complete and draft genomes of *Vibrio* spp. (n = 11627 in total), using PanACoTA (version 1.3.1 (20)), ran with the Singularity module. We used the methods 'prepare -s < species>' (where < species > was iteratively replaced with the most representative species of Vibrionacea: Vibrio, Aliivibrio, Enterovibrio, Photobacterium, Grimontia, Salinivibrio and Thaumasiovibrio, databases accessed in March 2022), with the options '–min 0 –max 0.4', for the MASH distance thresholds (21). We then used the method 'predict –prodigal' to syntactically annotate the genomes.

Overall strategy for detection of phage satellites

There are only a few experimentally verified satellites. This means that the sizes of the learning sets are insufficient for the use of machine learning methods to identify the elements at this stage. Instead, we made a curated annotation of a large set of known satellite elements and used them to iteratively identify core genes of each family of satellites. We then designed individual and customizable MacSyFinder (22,23) models that represent the genetic composition of the different phage satellite families (Figure 1 and Supplementary Figure S1). The models were used in MacSyFinder to identify occurrences of the putative satellites. MacSyFinder missed a few elements in certain genomic contexts or was unable to disentangle tandem occurrences of similar satellites. Hence, to improve the methods, we developed a post-processing script, which also provides an automatic classification of the satellite variants (Figure 1).

The design of the models for each satellite family is a necessarily manual process (see more details below), that started with an educated guess of the main core components, based on the literature review of known satellites. From these, we optimized the detection of satellites by iteratively adding (or removing) putative core components based on their high (or low) frequency across all the putative phage satellites that we detected (even if at this point there was no way to know if they were true phage satellites). This process was repeated until very few changes occured between iterations. The current set of core components was sufficient to accurately classify most of the known phage satellites of the corresponding family. Once these models were defined, we developed an approach, based on MacSyFinder, that automatically detects phage satellites in bacterial genomes. In the following sections, we describe in detail the key steps of both the model design and satellite detection process. The details associated with each family of satellites are given in the initial paragraphs of each section of the results, and the tables with all the satellites identified are given in File S2.

Modelling of satellite-like systems

We made a manual iterative enrichment and curation of the core (marker) components based on the analysis of genomic regions in bacterial genomes that could correspond to putative satellites. This resulted in MacSyFinder models that were used to automatically search for these elements in

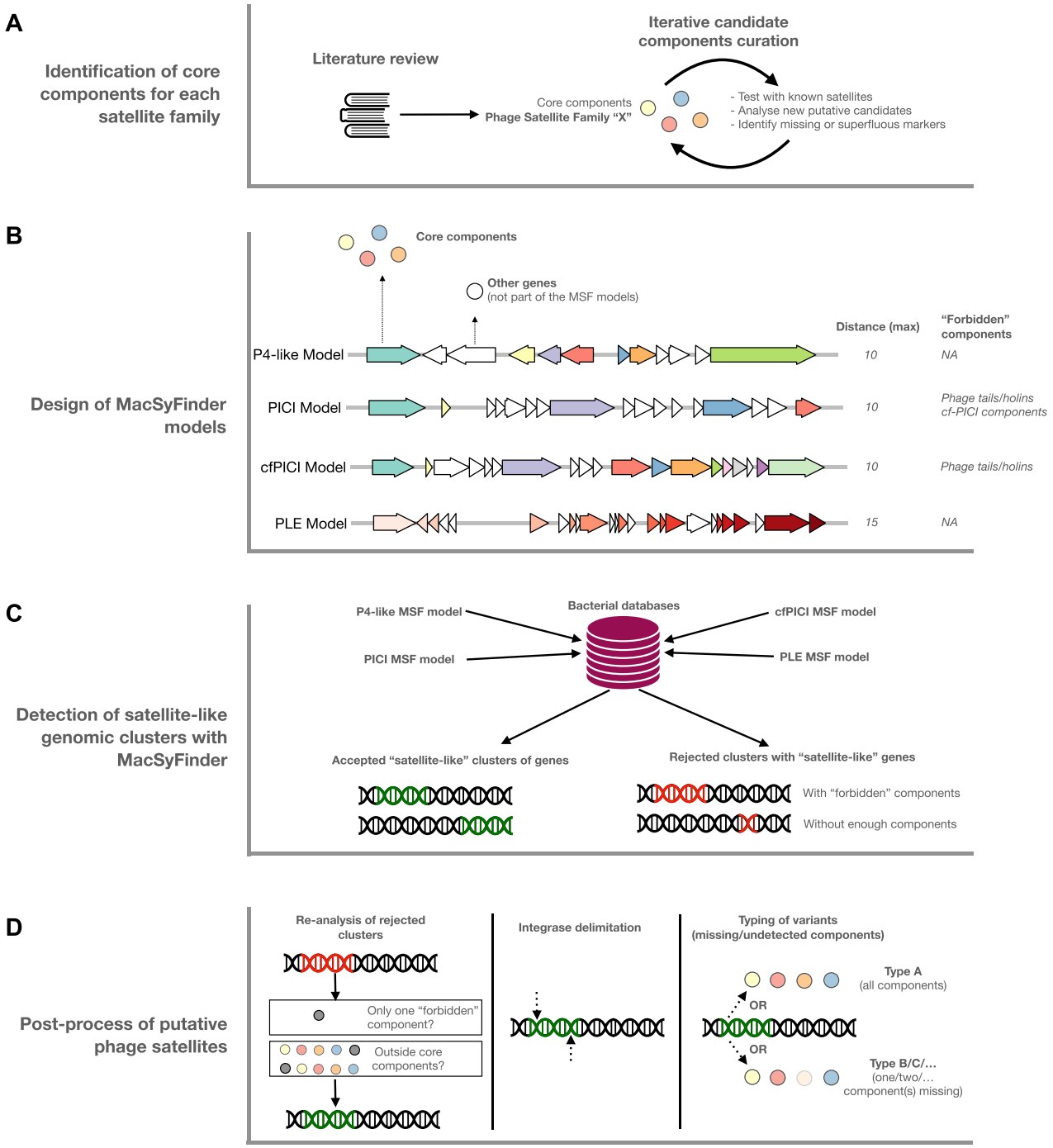

Figure 1. The different steps involved in the development and usage of SatelliteFinder. (**A**) Initial identification of putative core components of phage satellites from literature review and iterative search for associated genes in bacterial genomes. (**B**) Representative phage satellite genomes of the four different phage satellite families. Genes used as core components are shown as colors (colors across satellite genomes do not correspond to similar or equivalent components). Other genes in these specific representative genomes that are not core components are shown in white. These non-core components are not used to search for satellites. The maximum distance between components used in each case, as well as the forbidden genes used for each model, are shown at the right. Together, this information corresponds to the MacSyFinder models that are used in (**C**), to look for phage satellites in bacterial genomes using MacSyFinder. The resulting satellite-like clusters are the post-processed (**D**), resulting in the prediction, delimitation and classification (regarding the completeness) of putative phage satellites.

bacterial genomes. We outline the different steps involved in generating the phage satellites' MacSyFinder models below.

1. We collected genomic regions containing the pre-defined components (i.e. those identified from the literature of known phage satellites) at less than a pre-defined distance, to minimize the detection of components of tandem elements. For example, two components are clustered if they are less than X genes apart (15 for PLEs, 10 for the other families, see below for details on determining this maximum distance). We make a transitive clustering of the components, i.e. when one advances linearly in the genome sequence the cluster is closed and evaluated only when meeting a succession of more than X genes lacking a marker. If the cluster contains enough marker genes, i.e. it meets the minimal quorum, it is kept for further analysis. At this stage, we manually verified that the current models identified the known or previously proposed satellites and did not classify known phages as satellites. If known phages were mistakenly classified as satellites, we further refined the models, either by adding or removing components, or by including 'forbidden' components (see below for more details on the latter).
2. We took these putative satellite-like clusters and built their pangenome to identify the most abundant gene families in each phage satellite family. The pangenomes were built by clustering all the candidate proteins at a minimum of 40% identity, using mmseqs2 (24) (version 13-45111), with parameters –cluster_mode 1 and –min_seq_id 0.4 (all other parameters were left as default).
3. The resulting gene families were functionally annotated using PFAM (release 33.1) and bactNOG (25). Briefly, we used HMMER with an evalue cutoff of 10^{-5} and with a minimum coverage of 40% to find homologs of all PFAM and bactNOG profiles in the representatives of gene families of each satellite.
4. Sometimes a family that was not initially used as a marker was found to be present at high frequency in #2. The frequency threshold required to include a gene family as a core component depended on the number of elements in total, but it typically involved being present in at least 50% of the putative elements. In such cases, we checked if an adequate HMM profile was available in PFAM. If this was not the case, an HMM profile was built from the sequences that formed a gene family (see details below). In any case, the inclusion of novel profiles implicated re-starting the process (back to #1).
5. We tested if we should define groups of marker genes as 'exchangeable'. In such cases, MacSyFinder will fill the quorum of a marker if it identifies one of a set of protein profiles. For example, integrases of the Tyrosine recombinase and of the Serine recombinase families are often found as functional analogs in mobile genetic elements. To identify these exchangeable elements, we searched the literature or queried the known satellites for analogous components. We introduced these 'exchangeable' components in the MacSyFinder models using the corresponding tag, and re-started the process at #1.
6. We varied empirically the parameter of maximal distance between consecutive components (i.e. how further away from the rest of the cluster a gene should be in order to be accrued to the cluster) to test how it affects the method. Although we started from the typical distances between components in known satellites, when the analysis revealed that we should extend this distance because some frequent gene families were often found a bit further downstream, we adapted this parameter. If this increased the frequency of a gene family up to the point where it could be used as a marker, we started again at #1. In the cases presented in this study, a distance of 10 (for P4-like, PICI and cfPICI) or 15 (for PLE) genes was regarded as a good trade-off between identifying a few unusually long elements and preventing the frequent aggregation of several satellites (or other elements) into one cluster. This parameter is setup within each phage satellite model and can be modified by the user.
7. Sometimes we added components in the models to improve the discrimination between different families of satellites, or between satellites and prophages. In most cases, this was done by including 'forbidden' components. These are components that lead to the rejection of the element if they are present within it. We added forbidden components for those functions that are almost never found in one family of satellites. For example, tail and holin proteins are never (or very rarely) found in satellites and allow to distinguish them from prophages, and as such we include (respectively) 80 and 16 different profiles corresponding to these forbidden components. When novel forbidden markers were added, we started again the modelling at #1. In the current iteration of the models, forbidden components are used for PICI and cf-PICI. In both cases, we used profiles of phage holins and tails as forbidden elements, to avoid detecting phages as phage satellites. For PICI, we also used the portal, head-tail connector and head-tail adaptor of cf-PICI as forbidden components, to avoid the detection of cfPICI as PICI.

This iterative procedure resulted in a MacSyFinder model for each family of satellites. These models were used to systematically search for putative phage satellites in bacterial genomes. The MacSyFinder models for each satellite family are available within the Docker package of SatelliteFinder (https://hub.docker.com/r/gempasteur/satellite_finder).

Identification of markers and construction of HMM profiles

The first step in identifying novel satellites is to characterize the known ones and identify the genes that are most frequently associated with them (markers). We collected the satellites experimentally verified or proposed as homologs in previous publications and clustered their proteins by 40% protein sequence similarity (or 20% similarity for some PLE components PLEs, since the limited number of genomes resulted in some more diverse clusters not reaching the higher threshold). This revealed families of proteins that were the most frequent in a given family of satellite. The majority of these frequent components was adequately identified by

existing HMM profiles of the PFAM database. For this, we used HMMER and collected hits with maximum *e*-value of 10^{-3} and a minimum of 40% coverage as thresholds. Particularly for the case of PLEs, when no existing profile matched a frequent gene family, we built custom HMM profiles by aligning all sequences of the family with Clustal Omega (26) (Version 1.2.3) with default parameters, and then by using hmmbuild (default parameters) from hmmer 3.3.2 (27). The profile of Sid in P4-like satellites was previously constructed as detailed in (5). These profiles are available as Files S5–S22.

Identification of putative phage-satellites with MacSyFinder

We used MacSyFinder (22,23) (version 2.05rc) to provide a reproducible, shareable, and easily modifiable tool to identify phage satellites in bacterial genomes. Briefly, MacSyFinder searches for co-occurrence of the markers of each phage satellite family in bacterial genomes. The criteria for the identification of the occurrences of markers and for the acceptable patterns of co-occurrence can be defined by the user and that is what we call a model. MacSyFinder reports the cases with highest scores, namely where the largest co-occurrence of the different markers was found. For example, a genomic region with all markers gets a higher score than a genomic region with fewer markers.

Typically, one searches for these markers either using curated thresholds or by providing an *e*-value cutoff. Here, we lacked previous information on protein sequence diversity in the satellites and we tried to maximize the sensitivity of the models relative to this parameter. Hence, we used general and relaxed cutoffs (*e*-value <0.01 and coverage >40%, with parameters '–no-cut-ga –i-evalue-sel 0.01 –coverage-profile 0.4' in MacSyFinder), to detect distant homologs. The MacSyFinder model requires the identification of a number of markers and their co-occurrence. The need to respect a minimum quorum of co-localized components decreases the rate of false positives that could arise from the use of relaxed criteria of sequence similarity, because false positive satellites would require the random simultaneous co-localization of individual false positive markers. This co-localization would be extremely unlikely in most cases. Yet, a specific concern arises with degraded prophages that could resemble some satellites. These are discussed in the corresponding results section. The remaining parameters of MacSyFinder were left as default.

Post-processing of MacSyFinder results

The use of MacSyFinder alone allows to find most of the known or previously proposed satellites (Table S1). Yet, we noticed that a few novel elements were lost in some families (up to almost 8% of cfPICI elements, much less in other cases). This is caused by two features of the program that we corrected by post-processing the results.

1. Clusters of genes with a match to at least one forbidden profile are rejected. This feature is required to distinguish satellites with markers often found in phages from phages themselves, or to distinguish between different satellite families with many homologous core components. However, sometimes satellites and prophages are contiguous in bacterial genomes and the forbidden component is on the flanking element, not on the satellite itself. Hence, we post-process the results to include those discarded due to the presence of one single 'forbidden' component in the cluster (to allow for unknown variants) and those where the 'forbidden' component is outside of the cluster of components (prophages contiguous to satellites). These 'rescued' clusters are very rare for most satellite types (see Results section). They are specifically identified in the output of our scripts and in our analyses in the main text.
2. MacSyFinder outputs the largest possible cluster of markers of satellites, which may result in merging multiple satellites. It may also merge satellites with small contiguous mobile elements having an integrase. Our post-processing starts by handling the occurrence of multiple integrases and then focuses on tandem satellites. First, we search for the presence of multiple integrases (we assume there should be only one). If so, the algorithm chooses the one that is closest to the other (non-integrase) components. It may then eventually use another integrase as a starting point of a new set of components. This procedure may thus output several putative satellites from a single MacSyFinder cluster.

The MacSyFinder output lists the markers present in each putative satellite. For the analysis of the number and types of components present in the latter, we post-process the output to classify putative satellites into 'types': (A) have all (N) core components, (B) have $N-1$ core component, (C) have $N-2$ core components, and so on. These types are further categorized as 'variants' that correspond to the component(s) that are missing. We note that many Type B and C elements are complete and functional, since some correspond to elements that were experimentally verified, and many are very conserved. They may correspond to a variant of the prototypical satellite that either completely lacks a given marker component (e.g. due to gene loss or pseudogenization), has a non-homologous analog of the component, or has a diverged component that was not detected.

Genomic comparison of phage satellites with weighted gene-repertoire relatedness (wGRR)

We searched for sequence similarity between all proteins of phages and/or satellites using mmseqs2 (24) with the sensitivity parameter set at 7.5 to align all versus all proteins. The results were converted to the blast format and we kept for analysis the hits respecting the following thresholds: *e*-value lower than 0.0001, at least 35% identity, and a coverage of at least 50% of the proteins (since mmseqs2 searches for local similarity). The hits were used to retrieve the bi-directional best hits between pair of genomes, which were in turn used to compute a score of gene repertoire relatedness weighted by sequence identity (28):

$$wGRR = \frac{\sum_i^p id\,(A_i,\, B_i)}{\min\,(A,\, B)}$$

where A_i and B_i is the pair I of homologous proteins present in A and B, $id(A_i,B_i)$ is their sequence identity in the local alignment, and $\min(A,B)$ is the number of proteins of the

genome encoding the fewest proteins (*A* or *B*). wGRR is the fraction of bi-directional best hits between two genomes weighted by the sequence identity of the homologs. It varies between zero (no bi-directional best hits) and one (all genes of the smallest genome have an identical homolog in the largest genome). wGRR integrates information on the frequency of homologs and sequence identity. For example, when the smallest genome has 10 proteins, a wGRR of 0.2 can result from two identical homologs or five homologs each with a lower sequence similarity (40%). The hierarchical clustering of the wGRR matrix, and the corresponding heatmap, were computed with the *clustermap* function from the *seaborn* package (version 0.11.1, developed for Python 3.9), using the Ward clustering algorithm. The latter algorithm was also used to cluster the presence/absence of satellite-like components across all phage and satellite genomes.

Calculation of diversity of bacterial hosts

We assessed the diversity of the phage satellites' bacterial hosts using two measures. The species diversity (*S*) is the number of bacterial species where at least one phage satellite was identified. Since the genome datasets are very unbalanced, with some species accounting for a large fraction of genomes, the Species Diversity measure can misrepresent the true diversity of the hosts of satellites. Hence, we compute the Shannon's diversity index (*H′*) (29) for each phage satellite family. The index is calculated according to the formula:

$$H' = -\sum_{i=1}^{R} p_i \ln(p_i)$$

where *R* is the total number of bacterial species with at least one satellite, and p_i is the proportion of satellites found in the ith bacterial host species, in relation to the total number of satellites for the corresponding family (e.g. if there is a total of 500 elements, and 300 are found in *E. coli* genomes, $p_{E.coli} = 0.6$). Thus, a family of satellites where the vast majority of elements is located in only a few bacterial species will have a lower Shannon diversity index than a family of satellites that is equally spread across bacterial species.

Phylogenetic analysis

We aggregated in single fasta files all the protein sequences corresponding to either the regulatory, capsid or small terminase components of both PICI and cfPICI genomes. The sequences were aligned using mafft-linsi (30) (v. 7.490, default parameters) and the resulting alignment trimmed with clipkit (31) (v. 1.3.0, default parameters). We then used IQ-Tree (32) (v. 1.6.12) to build the phylogenetic trees, with the options –bb 1000 to run the ultrafast bootstrap option with 1000 replicates and –nt 6. The resulting tree files were visualized and edited using the v5 webserver of iTOL (33).

We used Coinfinder (version 1.2.0) (34) to analyse the frequency of association of different phage satellite families in the same bacterial genome. We used the core phylogeny of *E. coli* genomes, computed with PanACoTA (20). Briefly, the genomes of *E. coli* in our dataset were retrieved, filtered to remove very closely related genomes (MASH distance less than 0.0001), and then clustered using mmseqs2 with a minimal threshold of 80% identity in protein sequences. Within the pangenome of these 657 genomes there were 2107 families present in >90% of the genomes, which make the core genome. The core genome was aligned (for families with not more than a single gene per genome) using mafft-linsi, rendering one multiple alignment with 2 069 583 positions that was used to build a phylogenetic tree by FastTree 2.1 with model JC (35). Afterwards, we edited (i.e. rounded) the branch distance of very close nodes (<0.0001) to 0.0001 (1145 nodes out of 2630 in total), since Coinfinder detects these as branches with 0 distance. The resulting phylogeny was used as an input of Coinfinder, along with a file composed of the distribution of phage satellites across *E. coli* genomes. We used either the –associate or –dissociate options of Coinfinder to obtain the statistical significance of associating or dissociating families of satellites that infect the same bacterium.

Availability

We provide the MacSyFinder models and the customized python scripts to perform the abovementioned post-processing as a tool we call SatelliteFinder, that is available as a Docker package (https://hub.docker.com/r/gempasteur/satellite_finder) and also as a Galaxy server interface (36) (https://galaxy.pasteur.fr/root?tool_id = toolshed.pasteur.fr/repos/fmareuil/satellitefinder/SatelliteFinder/0.9). A brief summary on how to use both these approaches, as well as how to interpret the output of SatelliteFinder, is shown in File S3. The genomes (proteomes) of the satellite-like elements extracted from bacterial genomes and analysed in this manuscript are available in supplementary material (File S4).

RESULTS

P4-like satellites are frequently found in enterobacterial genomes

The P4 satellite is among the best studied satellites (11,37,38). It physically constrains P2 capsids to encapsidate its own DNA. Our previous work has shown that the P4-like family of satellites contains seven very conserved components (5). We used this information to build MacSyFinder models to detect P4-like satellites (see Methods). We searched for the co-occurrence of an integrase with six other components: Psu, Delta and Sid, which are involved in the hijacking of the capsid of the P2 helper phage; a regulatory protein, typically homologous to AlpA (although we also search for homologs of MerR or Stl as other possible regulators); Ash (also called ε), which inactivates the repressor of the helper phage, causing its induction; and α, a protein with primase and helicase activities that is required for P4 replication.

The P4 MacSyFinder model identified a similar amount (1054 vs 1037) of P4-like elements relative to our previous search in the same database (5). More than 93% of the most

complete elements (927) are strictly identical in both approaches (Jaccard similarity = 1). The remainder elements are in the same locations and only differ in terms of gene content. This is due to the ambiguity in the process of delimitation of P4-like satellites when they are flanked by two integrases (Figure S2). We used this model to search for P4-like elements in a much larger dataset of 21084 bacterial genomes, where the most abundant phyla are Proteobacteria (57%), Firmicutes (22%) and Actinobacteria (10%) (Figure 2, File S1). We more than doubled the number of putative P4-like satellites previously identified (2160). The majority (1621) of these elements encode all the seven core components (henceforth called Type A, Figure 2A and B), whilst 350 elements lacked one of them (Type B). The missing component may be absent, be non-identifiable by the protein profile, or may be replaced by a functional analog (see Materials and Methods). The most abundant of these variants lacks Psu (Type B#var06). Since Sid and Psu are structural homologs (39) it is possible that some variants of the former may compensate for the absence of the latter. There are 189 elements that lack two core components (Type C), most often ε and α (Type C#var01) or AlpA and α (Type C#var02). The vast majority of the putative P4-like phage satellites (93%) were detected in Enterobacteriaceae, a family that comprises ca 20% of all the bacterial genomes in the dataset. 35% of all the bacterial genomes from this family encode from one to three of these elements (Figure 2C and D). Other bacterial families with P4-like elements include Yersiniaceae (23% of the genomes with at least one element), where variants lacking Psu are prevalent, Pectobacteriaceae, Erwinaceae and Hafniaceae. All but one P4-like elements are integrated in bacterial chromosomes, with one outlier P4-like satellite integrated in a large plasmid. This confirms that these elements are usually not present in cells as plasmids.

Consistent with our previous analysis, the organization of the core components of P4-like satellites is conserved. Type A and the most frequent Type B variants encode the *psu-delta-sid* operon, followed by *alpA*, ε and α (Figure 2E and Figure S3A), with each component usually found in the same relative location (Figure S3B). We delimited the element between the integrase and its farthest core component, discarding those lacking an integrase. The resulting 2097 P4-like elements have a median size of 10Kb and a median of 11 genes (Figure 2F, G). A small minority of these (<2%) is larger (between 15 and 22 kb).

We measured the similarity between P4-like elements using weighted gene repertoire relatedness (wGRR, see Methods). Some elements are identical (peak at wGRR = 1 in Figure 2H), but most of them are only moderately related. The median wGRR is 0.42. We clustered them in relation to wGRR to assess their similarities (Figure 2F). There are two distinct sub-families within *Escherichia* genomes, and an additional large family including mainly elements found in *Salmonella* and *Klebsiella* genomes, but also in *Enterobacter* and *Citrobacter*. Other subfamilies include other clades such as *Serratia, Yersinia* and *Salmonella*. The subgroup of elements specific to *Salmonella* are all of Type C, as are the small family of elements in *Escherichia* genomes that form a very distinctive subfamily at the top of the matrix in Figure 2F. Many elements lack the same core genes and are associated with specific clades. This suggests that these are not defective elements. Instead, they seem to form distinctive variants (or subfamilies) of the P4 family. If the functions of the missing core genes in these variants are facultative, or if they can be complemented by other components remains unknown.

Although subfamilies tend to be associated with specific bacterial hosts, we also found some very similar elements in different species. This suggests horizontal transfer of P4-like satellites across distant bacteria. We found 3182 pairs of very similar elements in different bacterial species (4% of those with wGRR ≥ 0.9). Some very similar (wGRR > 0.8) pairs can also be found in different families (280 pairs, e.g. between Enterobacteriaceae and Hafniacea, or Erwiniaceae). Together, these results reinforce our previous findings of a large (and now even larger) family of P4-like phage satellites with a characteristic and conserved genomic organization and a broad host range.

Phage inducible chromosomal islands (PICI) are diverse and widespread across bacterial phyla

PICI include the *Staphylococcus aureus* pathogenicity islands (SaPI) that were extensively studied, as well as numerous other elements present in both diderm and monoderm bacteria (12,40). The described PICI have a conserved genetic organization and five core components found in almost all known elements: (i) integrase, (ii) regulation module (homolog to *alpA*, *merR* or *stl*), (iii) primase-replicase module, (iv) capsid morphogenesis (more frequent in PICI from Proteobacteria), encoding a protein that is thought to modify the morphology of the hijacked capsids to block the encapsidation of phage DNA, (v) small terminase subunit, responsible for redirecting the packaging of the capsid to the satellite's DNA. While other accessory genes are normally encoded by PICI (notably between the integrase and the regulation or the primase-replication module, or after the *terS* homolog), PICI typically do not encode other phage-like structural or lysis genes. We used the core components to detect PICI (Figure 1, Supplementary Figure S1B). Given the homologs between PICI, cfPICI (see below) and (pro)phages, we included in the PICI model several 'forbidden' components to discriminate them accurately from the others (see Materials and Methods): tail, holin, and some cfPICI components. The inclusion of the latter (specifically the components referring to portal, head-tail connector and head-tail attachment) prevents the PICI model to classify cfPICI as PICI, as there is an overlap between the core components used for both satellite families (Supplementary Figure S1B and C).

Our approach identified 1436 putative PICI, the vast majority (>99.9%) in chromosomes of Proteobacteria or Firmicutes (Figure 3A and B). 375 PICI (26%) were detected with the five core components (Type A), and 1061 (74%) with four (Type B). We note that a small number of them (31, 2%) were initially rejected by MacSyFinder due to the presence of one forbidden gene near (but outside) the cluster of PICI-like core components. They were recovered by post-processing the results (see Methods). The vast majority (97%) of the elements with all core components (Type A) were found in *E. coli* genomes. The other variants were

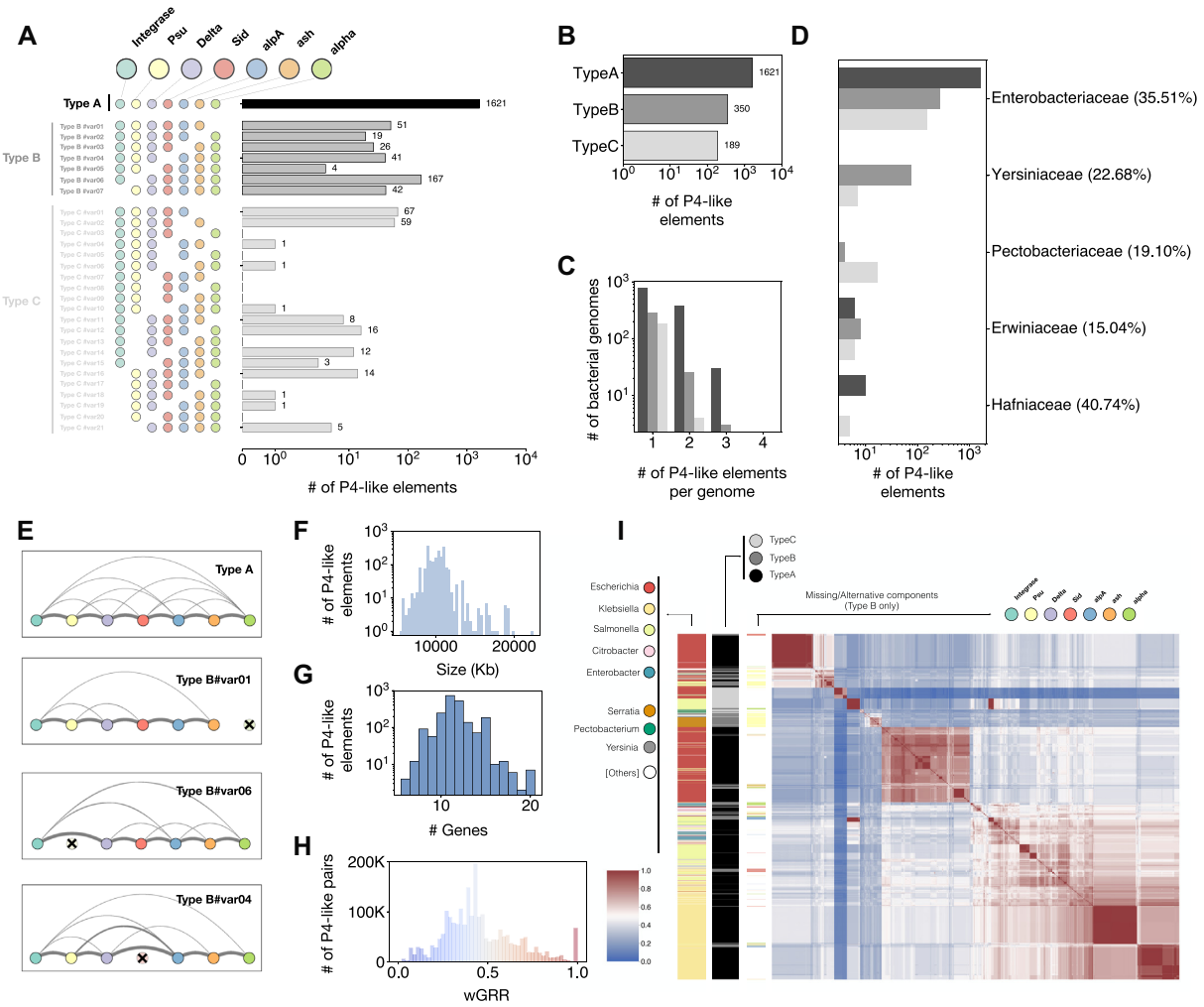

Figure 2. The abundance, genetic organization, bacterial hosts and genomic structure of the family of P4-like elements. (**A**) Number of the different variants of P4-like elements identified in bacterial genomes. (**B**) Total number of the different types of P4-like elements. (**C**) Total number of P4-like elements per bacterial genome. (**D**) Distribution of P4-like elements in bacterial families. The percentages in front of each family correspond to the proportion of genomes of that family where (at least) one P4-like element was inferred. (**E**) Genomic organization of the four most frequent variants of P4-like satellites. Nodes correspond to the different markers of the satellite (variants where the marker is absent have that indicated as a crossed-out node) and the edges between the nodes represent the frequency with which those two components are contiguous (but not necessarily adjacent). (**F**) Distribution of the sizes of the extracted genomes of P4-like elements. (**G**) Distribution of the number of proteins contained within each P4-like genome, for the elements detected. (**H**) Distribution of the pairwise wGRR values between all the P4-like genomes. (**I**) Symmetric heatmap of the matrix of the wGRR values ordered using hierarchical clustering. The colours follow the same code as in (**H**) with blue pixels representing low wGRR values (dissimilar genomes) and red pixels representing high wGRR values (similar genomes). The columns to the left of the heatmap indicate the bacterial species where the P4-like genome was detected, the Type (A, B or C) of the P4-like genome, and the component that is missing for given variants (exclusively for elements of Type B).

found across much more diverse bacterial hosts (Figure 3D), including in 66% of Mycobacterial genomes (including *M. tuberculosis*) and 35% of Staphylococcaceae genomes. Some of the latter were previously identified as SaPIs. They are known to lack the capsid morphogenesis gene typically found in Enterobacterial PICI because they rely in a different hijacking strategy (3). Thus, these variants are *bona fide* functional PICI, experimentally observed to be mobilized by helper phages. We also detected >6000 elements with three core genes (Type C). These may be functional satellites, but the small number of core genes increases the probability that they may be defective PICI, other mobile genetic elements, or just random aggregates of PICI-like functions (for instance, a typical P4-like satellite is classified as a Type C PICI because it encodes an integrase, AlpA and a primase/replicase). Hence, in order to remain conservative in our analysis, we focused on PICI-like elements of Type A and B.

PICI are present in many more species (190) than P4-like elements (81). These hosts are very diverse, including bacteria where phage satellites were not previously known to exist, and that are important in clinical and/or ecological settings. For instance, we detected putative PICI in *Acinetobacter*, *Bacillus* (as well as *Lactobacillus*), *Burkholderia*, *Clostridium*, *Rhodococcus* or *Sinorizhobium*. However, as most elements are found in a few (intensely sequenced) bacterial genus (e.g. *Escherichia*, *Mycobacterium* and *Staphylococcus*), the difference in diversity considering the overrep-

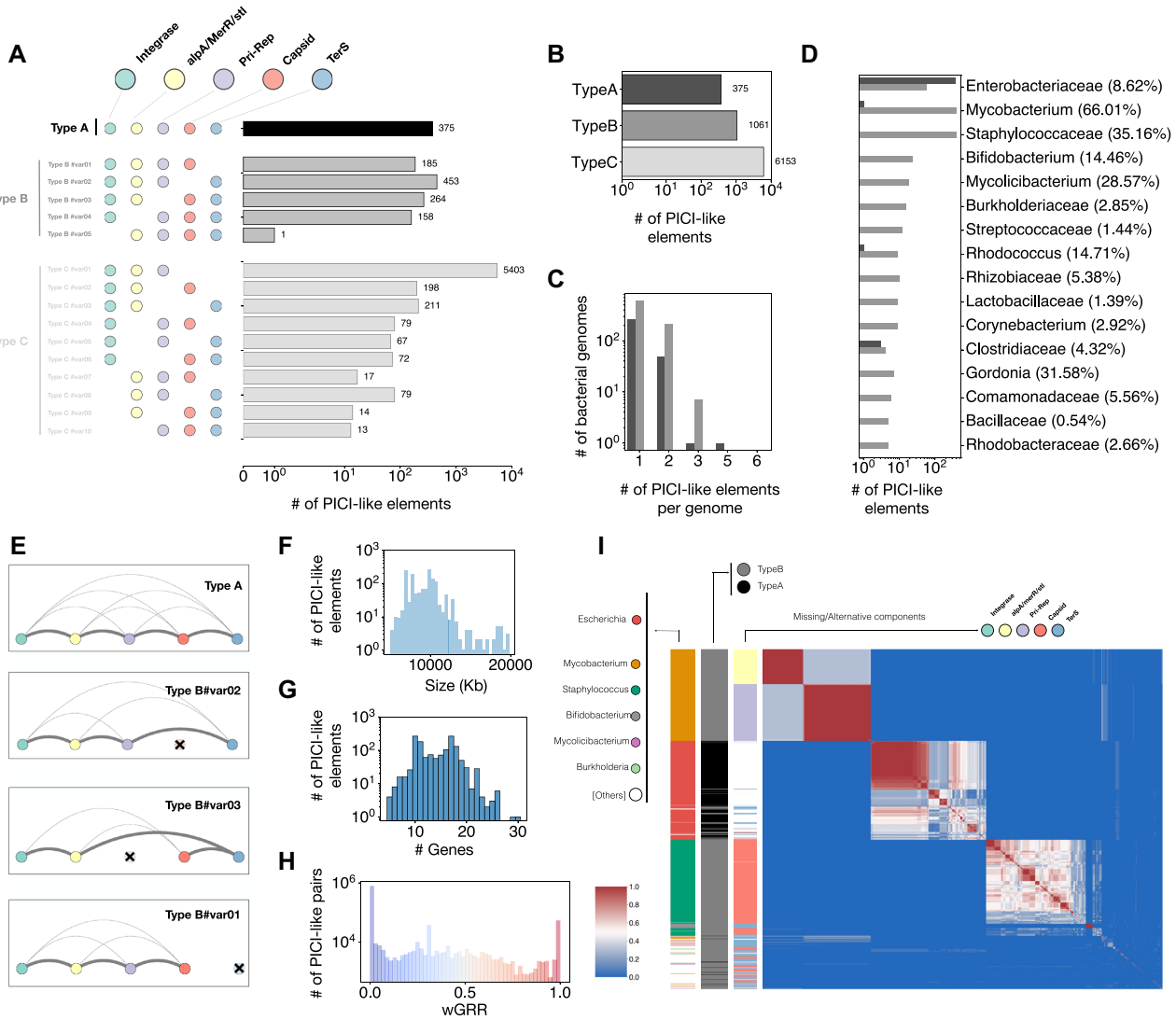

Figure 3. The abundance, genetic organization, bacterial hosts and genomic structure of the PICI family. (**A**) Number of the different variants of PICI-like elements identified in bacterial genomes. (**B**) Total number of the different types of PICIs. (**C**) Total number of PICIs per bacterial genome. (**D**) Distribution of PICIs of Type A or B in bacterial families. The percentages in front of each family correspond to the proportion of genomes of that family where (at least) one PICI was inferred. (**E**) Genomic organization of the four most frequent variants of PICIs. Nodes correspond to the different markers of the satellite (variants where the marker is absent have that indicated as a crossed-out node) and the edges between the nodes represent the frequency with which those two components are contiguous (but not necessarily adjacent). (**F**) Distribution of the sizes of the extracted genomes of PICIs. (**G**) Distribution of the number of proteins contained within each PICIs, for the elements detected. (**H**) Distribution of the pairwise wGRR values between all the genomes of PICIs. (**I**) Symmetric heatmap of the matrix of the wGRR values ordered using hierarchical clustering. The colours follow the same code as in (**H**) with blue pixels representing low wGRR values (dissimilar genomes) and red pixels representing high wGRR values (similar genomes). The columns to the left of the heatmap indicate the bacterial species where the PICI genome was detected, the Type (A or B) of the PICI, and the component that is missing for given variants (exclusively for elements of Type B). The putative elements that were initially rejected by MacSyFinder, and subsequently included by the post-processing automatic analysis, do not form a particular, segregated subcluster (Figure S6), suggesting they might be *bona fide* PICI.

resentation of PICI in certain bacterial taxa is less marked (Shannon index = 2.55 for hosts of PICI elements versus 2.14 for hosts of P4-like elements). Some bacterial genomes can have up to five PICI, even if most bacteria have one or two of these elements (Figure 3C).

The organization of the PICI core components is well conserved, as suggested by previous studies and mentioned above (12) (Figure 3E and Supplementary Figure S4). Only one of the most common variants shows a different order (Type B#var03, with a missing/unidentified primase-replicase), where the small terminase gene tends to be found before the capsid. We delimited the PICI from the integrase to the last identified core component (the element lacking the integrase was discarded). The resulting 1435 PICI have a median size of 9.5 kb (15 proteins), and only a few elements (17) have between 20 and 28 kb (Figures 3F and 3G).

PICI are much more diverse, as measured by the wGRR, than P4-like satellites ($p = 0$, two-sample Kolmogorov–Smirnov test). Their set of core components is smaller and most pairs of PICI have a very low wGRR (Figure 3H). The wGRR matrix groups PICI in four very distinct subfamilies, each predominantly associated with a bacterial clade: *Escherichia* (two sub-families), *Mycobacterium*, and *Staphylococcus* (Figure 3I). Most elements in Mycobacte-

ria tend to be very similar, forming two clusters with either an unidentified regulator or a primase-replicase. All the genomes of the putative satellites in *M. tuberculosis* (which are the majority of putative phage satellites identified in this taxon) are very similar to the previously described 'small prophage-like elements' PhiRv1 and PhiRv2 (41,42). Yet, other putative Mycobacterial phage-satellites are genetically distinct from the latter, and found across different species (e.g. in *M. abscessus*) (Figure S5). The *Staphylococcus* PICI lack a capsid modification gene, as previously described (12), and are split in many smaller subgroups. Those of *Escherichia* are very divergent and form smaller subgroups. There are also many small clusters of PICIs that each represent those few elements found in the genomes of other bacteria, and most of these PICI have four identified core components.

There are relatively few obvious cases of putative intraspecies transfer of PICI. Only 73 pairs of elements with a high wGRR are found in different bacterial species (0.1% of the total number of pairs with wGRR > 0.9, n = 60107). A large fraction is found in two *Staphylococcus* spp., although we do find some rare cases of putative transfer between more distant bacteria (e.g. *Acetivibrio* and *Tissierellia*). Thus, relative to P4-like satellites, PICI seem to be less frequently transferred across phylogenetically distant bacterial hosts. This may be a consequence of the presence of a majority of these elements in three very distantly related bacterial genera. Overall, these results uncover a plethora of very diverse PICI that are present in a large range of bacterial hosts.

Capsid-forming phage inducible chromosomal islands (cfPICI) are a novel and distinct type of PICI

The cfPICI are a novel family of satellites related with PICI, but with a unique trait: they assemble their own cfPICI-specific capsid (8). Yet, cfPICI are incapable of forming viable phage particles because they lack other structural genes that they hijack from the helper phage, e.g. holins and tail-associated proteins. The presence of genes encoding for structural components of the viral particle in cfPICI makes them more difficult to discriminate from prophages. For this reason, we defined profiles associated with phage tails, or phage holins, as forbidden components in the cfPICI model.

Five core components of cfPICI are homologous or analogous to the five core components of PICI, and in some cases the leftmost part of cfPICI (comprising the integrase, regulator and primase) were found to be exactly the same as PICI (8), suggesting they are indeed evolutionarily related. Some others are occasionally also found in PICI. This is the case of a nuclease (HNH) that is essential for phage head morphogenesis (and DNA packaging) in fully functional phages (43) and a head decoration module (a serine protease). We postulate that some of these genes might be used for the modification and stabilization of capsid morphology for phage capsids hijacked by PICI. However, there are several specific core components of cfPICI that allow to distinguish them from PICI: genes involved in the attachment of capsid to the hijacked tails (head-tail adaptor and head-tail connector), and a gene encoding the large terminase protein (*terL*) (Figure 1, Supplementary Figure S1C).

We detected 969 cfPICI, all but three in chromosomes. Among these cfPICI, 177 had all the 11 core components (Type A), 459 had 10 (Type B), and 333 had 9 (Type C) (Figure 4A and B). 73 of cfPICI (<8%) were initially rejected by MacSyFinder due to the presence of a nearby gene homologous with either a single tail or holin gene. They were retrieved in the post-processing step because the forbidden component is outside the cfPICI (see Materials and Methods). Type A cfPICI were exclusively found in Proteobacteria. They are very abundant in Enterobacteriaceae (13% of all genomes), and in Pasteurellaceae (8%) and Morganellaceae (7%) (Figure 4D). Variants of cfPICI within Firmicutes tend to have the capsid component merged with the prohead serine protease component (and therefore genes matching exclusively the capsid can be absent). As MacSyFinder reports the best scoring profile for each gene, the latter is chosen instead of the capsid profile(s). These cfPICI are frequently found in Lactobaciiliaceae (25%) and Enterococcaceae (25%), and rarer (<2%) in Bacillaceae and Streptococcaceae. Overall, cfPICI are found in more species than PICI or P4-like elements (136, Shannon index = 3.1), and are again present in several important species where phage satellites have not been detected (e.g. from the genus of *Bacillus*, *Bordetella*, *Citrobacter*, *Haemophilus*, *Pseudomonas* or *Xanthomonas*).

The genomic organization of the core components of cfPICI is very conserved, with the exception of two variants that are more diverse (Figure 4E and Supplementary Figure S7). We extracted the proteomes of the putative cfPICI, defined between the integrase and the farthest core component, after discarding five unusually large elements (>30 kb) and the 48 elements without an identified integrase. The remaining 916 putative cfPICI have a median size of 14 kb and encode a median of 19 proteins.

The gene repertoires of cfPICI are more similar than those of PICI, with a median wGRR of 0.2 and almost 10% of pairs with a wGRR higher than 0.8. Clustering the cfPICI by their wGRR reveals several subfamilies, usually associated with either monoderms (e.g. *Enterococcus* and *Lactobacillus*) or Proteobacteria (mostly *Escherichia*, *Klebsiella*, *Salmonella* and *Citrobacter*). This fits the previously obtained phylogeny of these elements (8). Within these subfamilies, cfPICI tend to be more similar between closely related hosts. The cfPICIs added by the post-processing script (e.g. with neighboring prophage genes) integrate the existing clusters, suggesting that they are valid elements (Figure S8). Although there is a strong association between cfPICI subfamilies and particular bacterial hosts, ca. 9% of the cfPICI pairs with a high wGRR (>0.9, $n = 36\,173$) were detected in different host species. For instance, some cfPICI of *K. pneumoniae* are very similar to those found in *Salmonella*, *Enterobacter* or *Citrobacter*. This suggests that, relative to PICI, cfPICI are potentially capable of disseminate across more phylogenetically distant hosts.

Phage-inducible chromosomal island-like elements (PLEs) form very homogeneous groups and are specific to *Vibrio cholerae*

PLEs were described in *V. cholerae*, where they play a critical role in the defense against the virulent phage ICP1 (6).

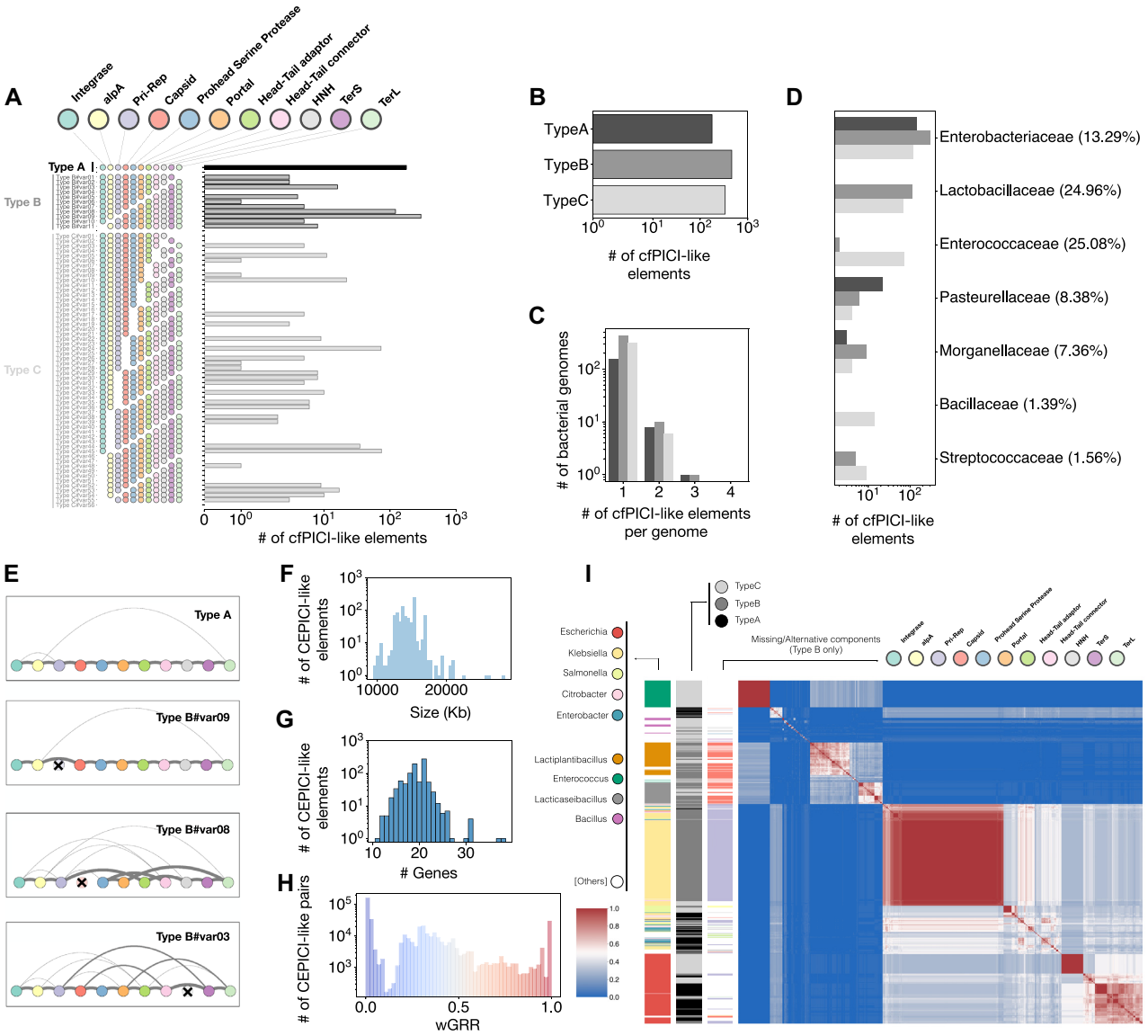

Figure 4. The abundance, genetic organization, bacterial hosts and genomic structure of the cfPICI family. (**A**) Number of the different variants of cfPICIs identified in bacterial genomes. This includes elements that were initially rejected by MacSyFinder but recovered with our post-processing analysis, and correspond to 38, 15 and 20 of Types A, B and C, respectively) (**B**) Total number of the different types of cfPICIs. (**C**) Total number of cfPICIs per bacterial genome. (**D**) Distribution of cfPICIs in bacterial families. The percentages in front of each family correspond to the proportion of genomes of that family where (at least) one cfPICI was inferred. (**E**) Genomic organization of the four most frequent variants of cfPICIs. Nodes correspond to the different markers of the satellite (variants where the marker is absent have that indicated as a crossed-out node) and the edges between the nodes represent the frequency with which those two components are contiguous (but not necessarily adjacent). (**F**) Distribution of the sizes of the extracted genomes of cfPICIs. (**G**) Distribution of the number of proteins contained within each cfPICI genome. (**H**) Distribution of the pairwise wGRR values between all the cfPICIs. (**I**) Symmetric heatmap of the matrix of the wGRR values ordered using hierarchical clustering. The colours follow the same code as in (H) with blue pixels representing low wGRR values (dissimilar genomes) and red pixels representing high wGRR values (similar genomes). The columns to the left of the heatmap indicate the bacterial species where the cfPICI genome was detected, the Type (A, B or C) of the cfPICI, and the component that is missing for given variants (exclusively for elements of Type B).

So far, all described PLEs are specific to *V. cholerae* (19) even if other putative satellites with homology to a few PLE genes were recently described in other *Vibrio* species (e.g. *Vibrio parahemolyticus*) (44). PLEs excise from the chromosome and package their genomes by hijacking ICP1. The cost for ICP1 is exacerbated by the acceleration of lysis promoted by PLEs after their packaging (45), which effectively halts the spread of ICP1 in the population.

To determine the core components of PLEs, we first selected the homologs present in at least three of the five prototypical PLE genomes (PLE 1 to 5 (6)). We treated differently the components most distant from the integrase because they are more variable; hence, we selected those found in at least two of the five prototypical PLEs. We used the core components for the iterative search of putative PLEs in the Vibrionaceae genomes (see Methods), which resulted

in the selection of a large number (15) of highly frequent markers for PLE. Some of these markers have a well-defined role in the PLE lifecycle: an integrase, a gene that represses the capsid morphogenesis of ICP1 (*capR*), a replication initiation protein (*repA*), a nickase that hampers the replication of the hijacked phage (*nixI*), and a gene that accelerates the lysis of the bacterial host cell (*lidI*). Other highly frequent markers of PLE to which we were able to assign a functional PFAM annotation include a protein with an HTH binding domain, which was previously described in PLEs (6); a sigma 70-like factor, a component of the specificity subunit of the bacterial RNA polymerase; and a profile with homology to a cyclin-dependent kinase-activating kinase (MAT1) suggested to be involved in nucleotide excision repair of damaged DNA (46). Seven other highly frequent markers (M1 to M7) were uncharacterized, and we were unable to annotate them using PFAM. Given the substantial variation in terms of presence/absence of these markers in the known PLE genomes (see Table S1), we used all the 15 markers to study the natural variation of this satellite family.

PLE are specific of a few Vibrio and are rare in our original dataset. To increase the sample size, we retrieved from Genbank all complete and draft genomes of Vibrionacea (11 627 genomes, see Methods). We detected 410 elements of Types A to I, i.e. with between all (Type A) and 7 (Type I) PLE markers (Figure 5A). Most genomes have a single PLE. Some of these types correspond to known variants of previously identified PLEs. Elements of Type A ($n = 238$) correspond to PLE1 and elements of Type B ($n = 38$), for which we only find a single variant, correspond to PLE5. PLE2 and PLE4 correspond to two different variants of Type D and PLE 3 corresponds to a variant of Type F (Supplementary Table S1). The more incomplete elements (Types G, H and I) tend to either lack or have highly distinct first or final half of the PLE markers we assembled, and it is likely that they result from assembling artifacts inherent to draft genomes. All the putative PLE-like satellites detected in the Vibrionaceae dataset were found in *V. cholerae* (in 12% out of 3446 total genomes for this species).

The core components present across the PLE variants are very diverse (Figure 5B), but the order of the components is extremely well conserved (Figure 5C). We extracted the region between the integrase and the furthest component (typically M4) in Type A elements. These regions have a median size of 17.7 kb (and 25 proteins). These elements tend to be genetically very similar, with >90% of the pairs having wGRR values higher than 0.9. Further, one can regroup all the PLE in 12 very homogeneous groups (with wGRR $\geq$ 0.9) (Figure 5F). While this may seem contradictory with the observation that several core genes are often missing, PLE differ from the other satellites in that a large fraction of genes are in the element's core genome. Some of these 12 groups were much more abundant than others, leading to a few very large clusters (Figure 5F). Overall, our results further confirm that PLEs are very distinctive from other satellites and have limited genetic diversity, forming highly related sub-families around the previously known PLE types.

Phage-satellite families form genetically distinct groups of mobile elements

All satellites exploit functional phages for mobilization, but the mechanisms involved in this process differ widely. This raises questions regarding the evolutionary origin of these elements: did they diversify from a single ancient satellite, or have they evolved multiple independent times? To understand the similarities between the different families of satellites, we analysed the co-occurrence of core genes from all satellite families across all the putative phage satellite genomes identified. For each satellite, we note the presence/absence of each core gene. The resulting binary matrix with all satellites was clustered (Figure 6) and revealed that three of the four families (P4-like, cfPICI and PLE), form well-separated and cohesive clusters of elements. PICI aggregated in multiple clusters, which is consistent with their high gene repertoire diversity (Figure 3I). Interestingly, the separation of satellites in different clusters is due to the combination of their markers, and not due to the presence or absence of a single one. For instance, AlpA is found in all P4-like, in many cfPICI and in some PICI. Moreover, the same protein can be matched by two different protein profiles of regulatory components (e.g. *alpA* and *merR*). In other cases, a single satellite genome has two regulatory genes, each matching a different protein profile. This analysis also occasionally identified satellites encoding components that are rare in their family of elements but very frequent (core) in another family of satellites. For instance, some cfPICI have a homolog of ε from P4, some P4-like satellites have a homolog of HNH from cfPICI, and some PLEs have a TerS homologous to that of PICI and cfPICI. These results show that the different families of satellites are clearly distinct, but they also suggest gene flow of core genes between satellite families.

A concern about the analysis is that it could mistakenly annotate phages as satellites, because they have homologous components. To test if this is frequently the case, we retrieved complete genomes of 3725 RefSeq phages and 15 558 complete or draft phage nucleotide sequences obtained from the NCBI database (see Materials and Methods). Importantly, these sequences were not used when modelling the satellites. We used this larger phage dataset as an input to MacSyFinder and found only 31 identified as satellites (14 as PICI and 17 as cfPICI). We then analyzed the presence of satellite-like markers in phages, in the same way that we did above for the satellites. Almost all phages have at least one homolog to a satellite core gene. This is expected because both often have an integrase and/or capsid-associated genes. Nevertheless, there are rarely more than a few of these core genes in common between phages and satellites. The former are the only elements with a consistent presence of holins and/or tail components. The clustering of the large binary matrix of presence of core genes (along with holins and tails) in satellites and phages shows that the latter form clusters well separated from those of satellites (Figure 6). These results confirm that our method discriminates well between satellites and *bona fide* phage sequences, and that these two types of elements are very distinct.

The previous results show that only a pair of satellites, PICI and cfPICI, has a lot of commonalities. We thus

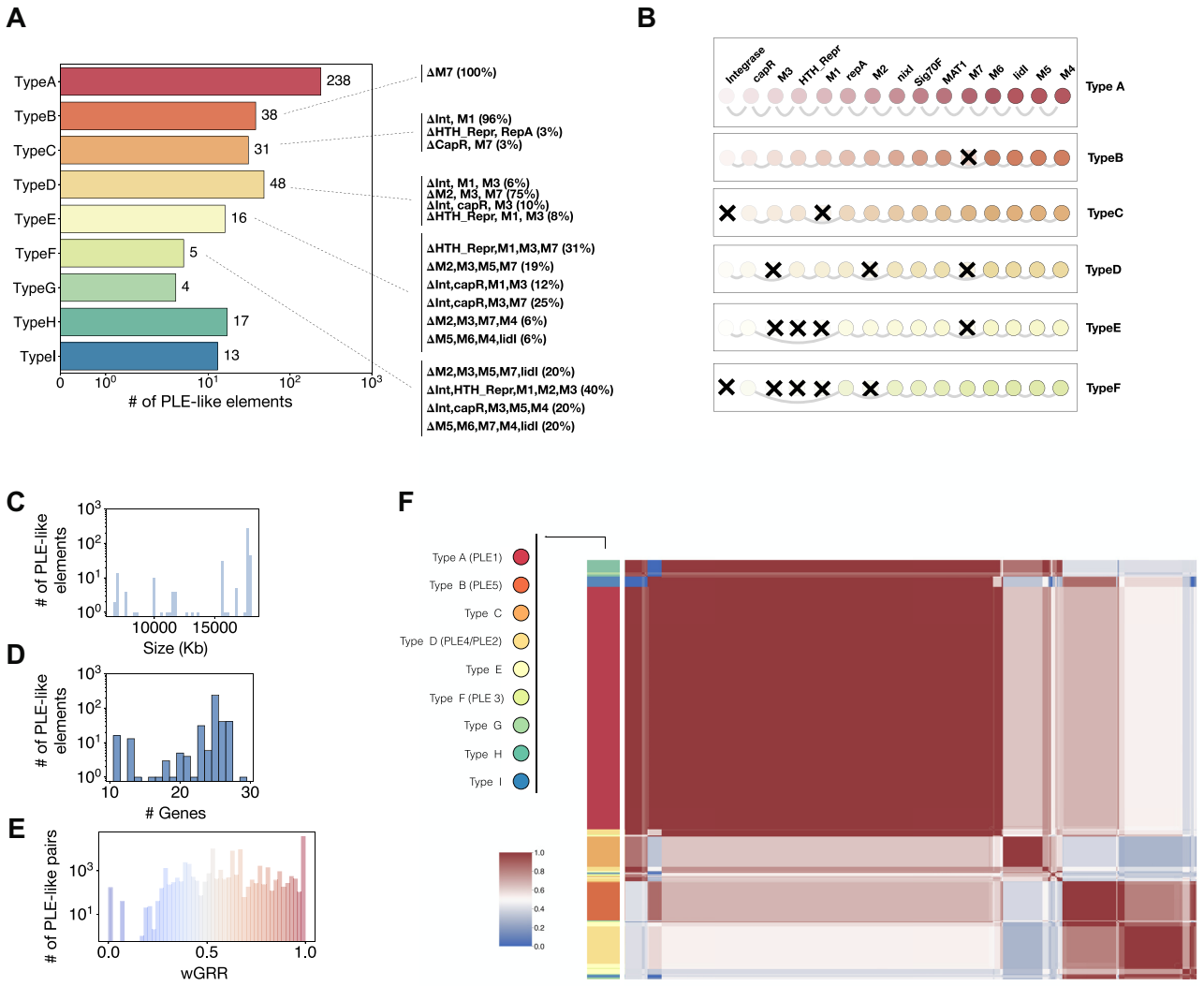

Figure 5. The abundance, genetic organization, genomic structure of PLEs. (**A**) Number of the different types of PLEs identified in Vibrionaceae genomes. Dashed lines in front of the bars indicate the variants within each type, more specifically which components are missing/undetected. The proportion of each variant is shown in parentheses. (**B**) Genomic organization of the most frequent variant for each PLE type. Nodes correspond to the different markers of the satellite (variants where the marker is absent/unidentified have that indicated as a crossed-out node) and the edges between the nodes represent the frequency with which those two components are contiguous (but not necessarily adjacent). (**C**) Distribution of the sizes of the extracted genomes of PLEs. Although we extracted genomes for all identified sets, we do not use those that are present across multiple contigs (1.2%) to account for the distribution in genome size, as the precise genomic locations (and relative distances) of the proteins would be unreliable. (**D**) Distribution of the number of proteins contained within each PLE genome. (**E**) Distribution of the pairwise wGRR values between all the PLE genomes. (**F**) Symmetric heatmap of the matrix of the wGRR values ordered using hierarchical clustering. The colours follow the same code as in (E) with blue pixels representing low wGRR values (dissimilar genomes) and red pixels representing high wGRR values (similar genomes). The column to the left of the heatmap indicate the type of PLE (in parenthesis, the prototypical PLEs that are classified with a similar type).

assessed the evolutionary relationships in this pair in particular, as the two families of satellites share several core components. We tested if SatelliteFinder is able to accurately distinguish them. First, no elements were simultaneously identified by the cfPICI and PICI models. Second, no PICI satellites were identified when searching for them directly in the dataset of cfPICI genomes. Finally, no cfPICI was identified when searching for them directly in the PICI genomes. This suggests we can discriminate them accurately. To confirm this, we quantified the genome-wide similarities between PICI and cfPICI, by computing the wGRR between them. The clustering of the wGRR values revealed little to no mixing between the major clusters of these two types of satellites (Supplementary Figure S9). Hence, these elements are well separated. This fits our previous work on the phylogeny of the capsid and TerL showing that these components of cfPICI emerged three times independently from phages (8).

We then built phylogenetic trees for four homologous core components present in both PICI and cfPICI: the transcriptional regulator, the primase-replicase gene, the capsid gene (or capsid-modification gene in PICI) and the small terminase. This revealed contrasting results. On one hand, the trees of the transcriptional regulators and of the

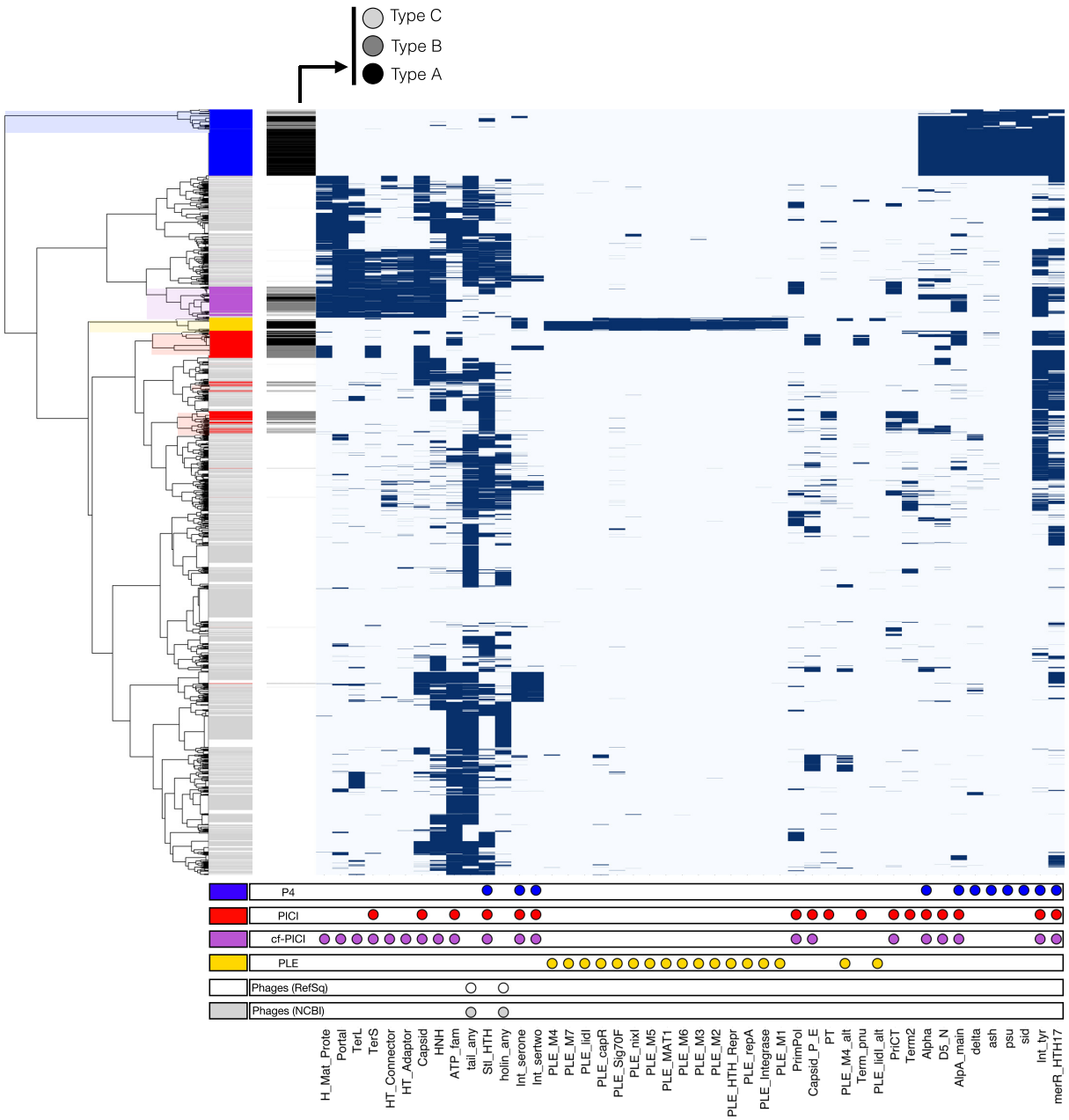

Figure 6. Pattern of presence/absence of the different satellite markers across all phage and putative phage-satellite genomes. Hierarchical clustering, using the Ward algorithm, of each phage or phage-satellite genome (row) assessed for the presence of a given phage satellite marker (column, at least one homolog gene with an *e*-value of at most 0.01 and minimum coverage of 40%). For each genome, if a homolog for a marker is present, the cell is shown as blue, otherwise its absence is shown as an empty cell. For the phage-specific markers (holins and tails) the total number of profiles (16 and 81, respectively) is summarized in a single binary value (i.e. if the genome has an homolog of any of the profiles used for each component, it is marked as 1, otherwise it is marked as 0). The markers used by SatelliteFinder to detect each phage satellite family are shown below the matrix as circles, as are the phage holins and tails. The columns on the right of the matrix indicate (from right to left): the family of the phage-satellite genome corresponding to each row; and the Type of each satellite genome (limited to Types A, B and C, phages from RefSeq are shown as white and those from NCBI are shown in grey). The clusters that are mostly composed of phage satellites are indicated as color shaded branches in the dendrogram on the left.

primase-replicase are strongly paraphyletic (Figure 7A and B), suggesting gene flow between the two families of satellites (or intermingled evolutionary history). On the other hand, the capsid (Figure 7C) and small terminase genes (Figure 7D) separate almost perfectly PICI from cfPICI. This suggests that some functions are more likely to be exchanged between different types of satellites. Alternatively, the integrase-proximal genes may constitute a functional module that might be involved in the cross-regulation of (potentially similar) helper phages. These results confirm that the first half of the PICI and cfPICI satellites have several homologs, which suggests a common evolutionary history for the presence of these components in satellites. In conclusion, these are two different families of satellites

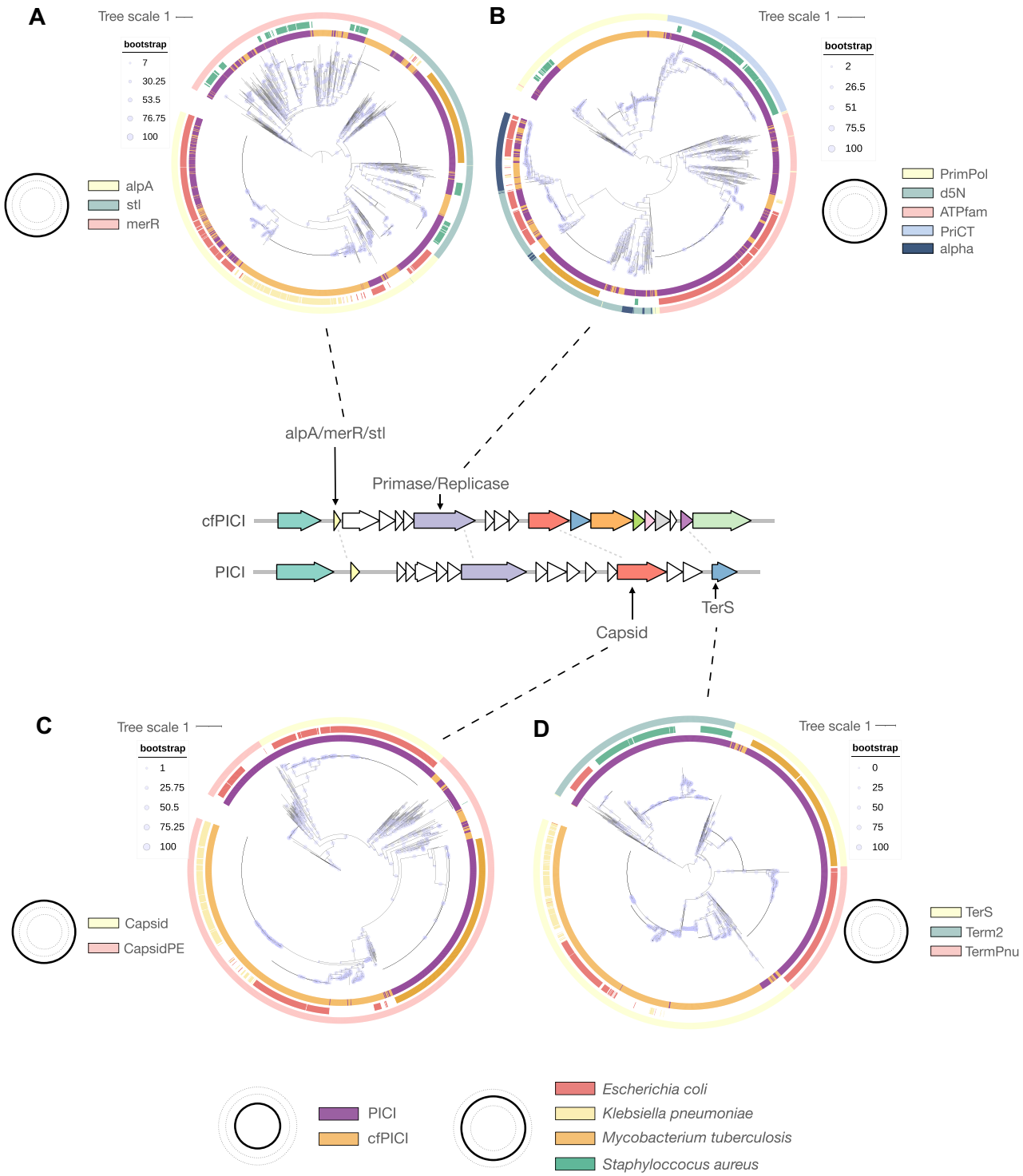

Figure 7. Phylogenetic trees of four of the prototypical components of PICI and cfPICI. (**A**) Tree of the regulators of cfPICI and PICI. (**B**) Tree of the primase-replicase components of cfPICI and PICI. (**C**) Tree of the capsid-like components of cfPICI and PICI. (**D**) Tree of the small terminase components of cfPICI and PICI. In both A, B, C and D, the outer circles indicate (from inside out) the family of satellites (PICI in purple, cfPICI in orange); the most frequent bacterial host species of the phage-satellites (less frequent host species are shown as white spaces); and the profile associated with the specific component (AlpA, MerR or StI for the regulator in A; the five different profiles used to detect a primase-replicase in B; the two profiles used to detect capsid-associated components (capsid or capsidPE) in C; and the three profiles used to detect a small terminase in D, see Supplementary Figure S1 for more details).

with a common region, and where part of the hijacking modules (those that *de facto* distinguish PICI from cfPICI) have evolved independently.

Phage-satellites of different types co-occur in bacterial genomes

Finally, since the families of satellites can be separated accurately, we assessed if multiple phage satellites, each belonging to a different family, could co-integrate the same bacterial genome, or if they mostly exclude each other. PLE never co-occur with other satellites, which is justified by the narrow bacterial host range of its helper phage. We analysed the associations of the other three families of satellites in *E. coli* genomes using Coinfinder (34) (see Methods). This software tool examines the presence/absence of pairs of genes across a phylogeny to determine if their relationship is coincidental, meaning that these genes are observed together or apart more often that would be expected by chance. We find that satellites of the P4-like, PICI and cfPICI families co-occur less than expected within *E. coli* hosts, as they are significantly dissociated (Figure 8). Nevertheless, we found that a few hundred bacterial genomes have at least one P4-like and one PICI (227 genomes) or a P4-like and a cfPICI (379 genomes). The former combination is mostly found in *E. coli* (Figure 8) or *Shigella boydii* genomes, while P4-like and cfPICI satellites tend to co-integrate a more diverse set of hosts, from *E. coli* to *K. pneumoniae*, *Citrobacter freundii* or *Yersinia enterolitica*. Combinations of PICI and cfPICI are less common, and we found them in only 47 bacterial genomes. Impressively, 31 *E. coli* genomes have at least one element of each of the three families of satellites (P4-like, PICI and cfPICI, Figure 8). Hence, these results show that, although a segregation of satellite families across different hosts might be expected, different families often co-exist within single bacterial genomes.

DISCUSSION

In spite of the impact of satellites in phage reproduction and in the transfer of adaptive traits among bacteria, there was little information in the literature on their composition and number. We were able to leverage previous curated analyses of a few dozens of such elements to build a tool—SatelliteFinder—that systematically and reproducibly identifies phage satellites in bacterial genomes. This approach revealed numerous novel satellites, highlighting their relevance in nature. Nevertheless, it has some limitations. First, the existence of few examples of experimentally validated satellites means that it is not possible to accurately evaluate our classification. We overcame this by using an iterative cycle of enrichment and curation of satellite markers, but this also means that the phage-satellite models we propose must be regarded as a first educated attempt to characterize each family. Interested users can easily modify MacSyFinder models by changing one single text file. This will facilitate the search for novel variants of known satellites and to add novel types of satellites. Second, the presence of mobile genetic elements in the close vicinity of phage satellites can affect the identification of the latter. For instance, multiple contiguous phage-satellites could be identified as an overly large single satellite and a neighboring phage may lead to the exclusion of a valid satellite because of more than a single nearby phage-like marker. The post-processing automatic analysis of MacSyFinder's output solves these issues only partially. For instance, while this manuscript was being submitted, a preprint showed that satellites can integrate inside prophages (47), which poses an even more difficult scenario to accurately distinguish these elements from prophages. Future work will be needed to assess the ability of our approach to correctly assign such cases. Third, we assume that satellites are delimited between the two furthest (identified) components. This may result in an underestimation of the size of the satellite, as well as their genomic repertoires. For instance, some accessory genes in PICI, namely genes involved in anti-phage defense, are found between the attachment site and the integrase (10). Fourth, we cannot ascertain if all satellites are functional. One would expect that most elements with the full set of core genes are functional. But even the other variants are highly conserved, and a few were experimentally validated, suggesting that many of them might be functional. Fifth, our approach is sensitive to the mis-annotation of small genes as pseudogenes. For instance, in our previous analysis, we inferred that a large number of Type B P4-like satellites had a pseudogene of *alpA*. However, this variant is very rare in the current analysis, because the most recent RefSeq database annotates *alpA* correctly. Finally, the PLE analysis was done with draft genomes where the phage satellites might be split across different contigs, erroneously suggesting that some elements are either missing or have alternative core components. This seems to be the case for the less complete PLE variants (Types H and I) that had homology to either the first or the last 'half' of the PLE model. This is not an issue when using complete genomes, as was the case for the analysis of P4-like, PICI and cfPICI.

Both the commonalities and uniqueness of the different families of phage satellites provide insights on their function and evolution. Among the key functions of satellites one finds those associated with integration, regulation, replication, and subversion. Integrases are core genes of all satellites because all elements are integrated in the chromosome. Regulatory components are also present in almost all satellites, and they are much more satellite-specific than integrases. It has been suggested that AlpA (or its functional analogues) mediate the cross-regulation between satellites and helper phages (12,16). The potential gene flow suggested by the mixed phylogenies indicates that there might be functional compatibility, both within and across satellite families (i.e. one regulator can be exchanged by another). It also raises the possibility that different satellites could exploit the same phages, independently of the satellites' hijacking strategy. Hence, regulators might be one of the best candidates to understand the evolution of satellites as a large family of elements. Another candidate could be the primase-replicase component(s), which are present in all the families, but the divergence or lack of sequence similarity between them suggests that they are analogs instead of homologs. Other components seem to be more specific to each family of phage satellites. The Psu-Delta-Sid operon of P4-like phage satellites performs a unique and conserved helper subversion strategy; the capsid assembly and head-

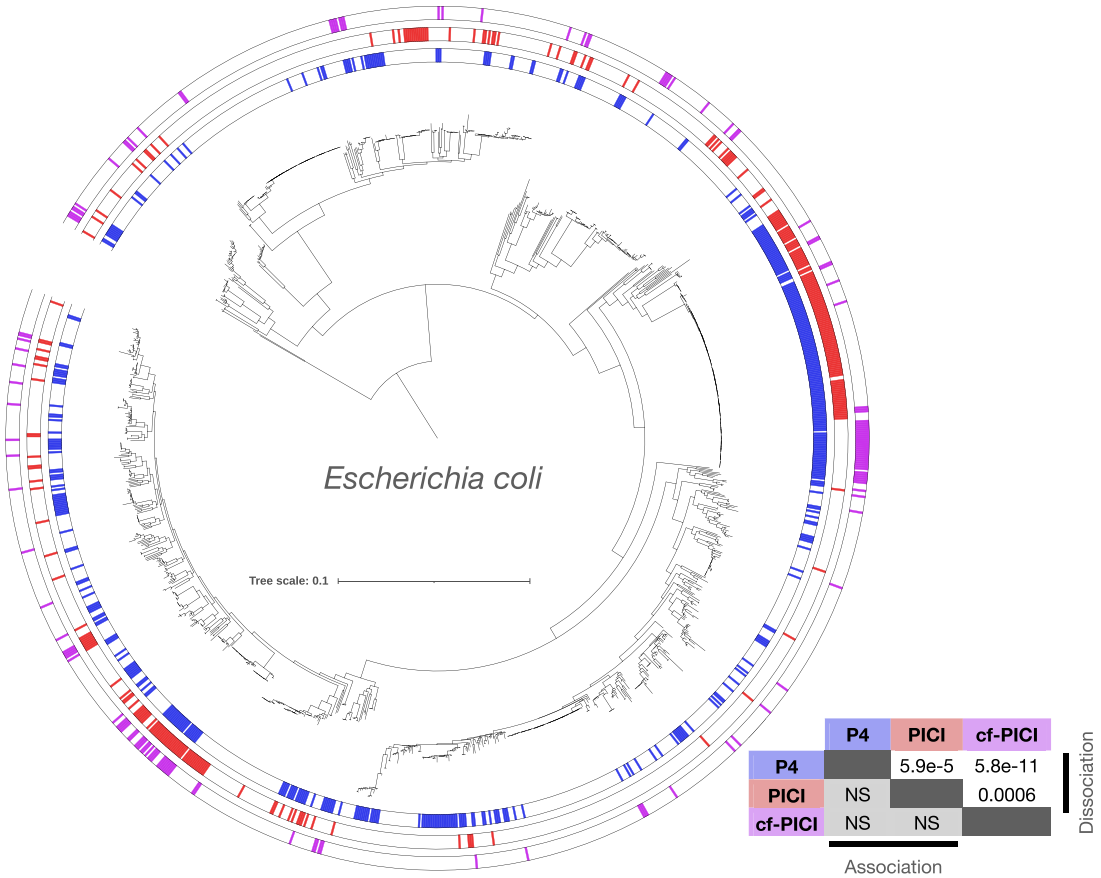

Figure 8. Distribution of P4-like, PICI and cfPICI in the genomes of *Escherichia coli*. The three circles around the core phylogeny of the *E. coli* indicate the presence (color) or absence (white) of at least one phage satellite, for each of the three families. The table indicates the significance value computed by Coinfinder for associations or dissociations between the three phage satellite families, within individual bacterial genomes (NS = non-significant).

tail adaptor genes of cfPICI means that this is the only satellite known so far that hijacks only part of the helpers' virions; and PLEs have evolved genetic machinery to not only subvert a specific incoming virulent phage, but also to kill its bacterial host upon excision. Interestingly, this strategy might also be used by some PICI, that were recently described to encode an abortive infection system (10), and P4-like satellites can also encode anti-phage defense systems (e.g. retrons) (9). Hence, while the overall strategies (of subversion, replication or anti-phage defenses) of the different families of satellites might seem similar, they occur through different genes and mechanisms, and are likely to have evolved multiple times.

Novel, and experimentally testable insights into the different core functions of phage satellites can also come from the presence/absence and organization of their core components. The conserved genetic organization of most satellites, including its variants, suggests the existence of tight relationships between contiguous core components and conserved programs of gene expression. Certain variants lack core components and form specific clades, thus suggesting they might be functional. If so, this would be an indication that these components are facultative. For instance, PICI of Type A represent a sub-family that relies on capsid modifications to hijack their helpers, while those of Type B do not require such a function. Psu-less variants of P4-like satellites are also frequent and form sub-families. One of these is associated with a specific bacterial clade (Serratia), suggesting that its function is either unnecessary or complemented by other components (e.g. Sid), and might have evolved within the bacterial species and in the context of its prophages. Other variants are rare and integrated into existing subfamilies of more complete types. These cases could represent recent loss of core components, that result in defective variants.

The different families of satellites are strikingly diverse in their abundance, taxonomic distribution, genetic composition, and genetic diversity. All of these might be suggestive of the ecological conditions that underlie the establishment of the tripartite relationships between bacteria, phages and their satellites. For instance, the reduced diversity and narrow bacterial taxonomical range of PLEs might result from the high conservation of ICP1 making it unlikely to infect (and thus transfer PLE to) other bacterial species (48). However, since PLEs were not described to exploit other phages, virulent or lysogenic, this also suggests that the selective pressure of ICP1 on *V. cholerae* might have created the conditions for the tight and highly specialized function of PLEs in the ecology and evolution of this bacterial pathogen. Other satellite families show a much higher

genetic diversity. P4-like satellites are found across many Enterobacteria and PICI and cfPICI are present across different phyla. It remains to be uncovered whether this taxonomic spread results from a promiscuous relationship between these satellites and their broad host-range helper phages (as our data suggests it is the case for some P4-like satellites), or from the diversification of very ancient versions of these satellites within each bacterial clade. Our previous results suggest that at least cfPICI may have emerged separately in Firmicutes and Proteobacteria (8). Ongoing work will help to solve the question of the origin of satellites.

Many bacterial genomes have multiple satellites of the same family. This creates an interesting context for interactions between these elements. One recently described example of satellite-satellite interactions involves a specific PICI (SaPI3) that is induced not by prophages, but instead by other co-integrated PICI (49). Furthermore, individual bacterial genomes often carry satellites of different families. We observed that these elements tend to show patterns of avoidance, i.e. the presence of one is associated with a lower probability of the presence of another. This suggests the existence of competitive or antagonistic interactions between phage satellites of different families. The high frequency of prophages, satellites and anti-phage defense systems in phage satellites (6,9,10) highlights the complex networks that dictate the emergence and maintenance of these elements that shape the fitness and survival of their bacterial hosts.

Our results reinforce the idea that phage satellites play an important role in the microbial world. Even if our approach was conservative, due to the requirement of many core genes common to known satellites, we detected ca. 5000 phage-satellites in bacterial genomes. This number is huge, given the little we know about the distribution and diversity of these elements. There are even more elements that we excluded because they lacked too many core genes relative to the known satellites (e.g. we found more than 6000 Type C PICI elements). These elements contain several hallmarks of phage-satellites, *e.g.* AlpA or packaging proteins, which suggests there may be many other, still undescribed, families of satellite in bacterial genomes. Such elements may use novel exciting mechanisms for replication, sensing, or phage hijacking. Many elements in marine bacteria have recently been proposed to be phage satellites (17,18), and other some 'incomplete' PLEs were recently described in Vibrionacea other than *V. cholerae* (44). Considering that half of the bacteria have at least one prophage (50) and that we identified satellites in a much smaller number of bacterial genomes, it is very likely that this is the beginning of the characterization of a vast diversity of phage satellites. SatelliteFinder allows to easily add or modify models for satellites. It allows to experiment combinations of both known and hypothetical marker genes, which will be key to identify novel putative satellites for experimental verification.

DATA AVAILABILITY

The bacterial and phage genomes, as well as most profiles used to detect the core components of phage satellites, are publicly available. For the core components without public HMM profiles, we include the custom profiles as Files S5–S22. The models used for MacSyFinder are also available MacSyModels in the public repository. The additional custom Python scripts to post-process the output of MacSyFinder are included in the Docker image at (https://hub.docker.com/r/gempasteur/satellite_finder).

SUPPLEMENTARY DATA

Supplementary Data are available at NAR Online.

ACKNOWLEDGEMENTS

We thank Kim Seed for comments and suggestions on earlier versions of the manuscript, Graham Hatfull for helpful discussion regarding the PhiRv1 and PhiRv2 elements in *M. tuberculosis*, and Bertrand Néron and Fabien Mareuil from the Institut Pasteur's Bioinformatics and Biostatistics Hub for help in the development of the Docker and Galaxy version of SatelliteFinder.

FUNDING

Equipe FRM (Fondation pour la Recherche Médicale) [EQU201903007835]; Laboratoire d'Excellence IBEID Integrative Biology of Emerging Infectious Diseases [ANR LBX-62 IBEID AAP BOURSE S2I ROCHA]; this work used the computational and storage services (TARS cluster) provided by the IT department at Institut Pasteur, Paris. Funding for open access charge: Laboratoire d'Excellence IBEID Integrative Biology.
Conflict of interest statement. None declared.

REFERENCES

1. Fernández,L., Rodríguez,A. and García,P. (2018) Phage or foe: an insight into the impact of viral predation on microbial communities. *ISME J.*, **12**, 1171–1179.
2. Touchon,M., Moura de Sousa,J.A. and Rocha,E.P. (2017) Embracing the enemy: the diversification of microbial gene repertoires by phage-mediated horizontal gene transfer. *Curr. Opin. Microbiol.*, **38**, 66–73.
3. Novick,R.P., Christie,G.E. and Penadés,J.R. (2010) The phage-related chromosomal islands of Gram-positive bacteria. *Nat. Rev. Microbiol.*, **8**, 541–551.
4. Penadés,J.R. and Christie,G.E. (2015) The phage-inducible chromosomal islands: a family of highly evolved molecular parasites. *Annu. Rev. Virol.*, **2**, 181–201.
5. Moura de Sousa,J.A. and Rocha,E.P.C. (2022) To catch a hijacker: abundance, evolution and genetic diversity of P4-like bacteriophage satellites. *Philos. Trans. R. Soc. B Biol. Sci.*, **377**, 20200475.
6. O'Hara,B.J., Barth,Z.K., McKitterick,A.C. and Seed,K.D. (2017) A highly specific phage defense system is a conserved feature of the Vibrio cholerae mobilome. *PLoS Genet.*, **13**, e1006838.
7. Fillol-Salom,A., Bacarizo,J., Alqasmi,M., Ciges-Tomas,J.R., Martínez-Rubio,R., Roszak,A.W., Cogdell,R.J., Chen,J., Marina,A. and Penadés,J.R. (2019) Hijacking the hijackers: *Escherichia coli* pathogenicity islands redirect helper phage packaging for their own benefit. *Mol. Cell*, **75**, 1020–1030.
8. Alqurainy,N., Miguel-Romero,L., Moura de Sousa,J., Chen,J., Rocha,E.P.C., Fillol-Salom,A. and Penadés,J.R. (2023) A widespread family of phage-inducible chromosomal islands only steals bacteriophage tails to spread in nature. *Cell Host Microbe.*, **3** , 69–82.
9. Rousset,F., Depardieu,F., Miele,S., Dowding,J., Laval,A.-L., Lieberman,E., Garry,D., Rocha,E.P.C., Bernheim,A. and Bikard,D. (2022) Phages and their satellites encode hotspots of antiviral systems. *Cell Host Microbe*, **30**, 740–753.

10. Fillol-Salom,A., Rostøl,J.T., Ojiogu,A.D., Chen,J., Douce,G., Humphrey,S. and Penadés,J.R. (2022) Bacteriophages benefit from mobilizing pathogenicity islands encoding immune systems against competitors. *Cell*, **185**, 3248–3262.
11. Christie,G.E. and Calendar,R.L. (2001) P4-like satellite viruses. In: Tidona,C.A., Darai,G. and Büchen-Osmond,C. (eds). *The Springer Index of Viruses*. Springer Berlin Heidelberg, Berlin, Heidelberg, pp. 1288–1292.
12. Fillol-Salom,A., Martínez-Rubio,R., Abdulrahman,R.F., Chen,J., Davies,R. and Penadés,J.R. (2018) Phage-inducible chromosomal islands are ubiquitous within the bacterial universe. *ISME J.*, **12**, 2114–2128.
13. Briani,F., Dehò,G., Forti,F. and Ghisotti,D. (2001) The plasmid status of satellite bacteriophage P4. *Plasmid*, **45**, 1–17.
14. Canchaya,C., Desiere,F., McShan,W.M., Ferretti,J.J., Parkhill,J. and Brüssow,H. (2002) Genome analysis of an inducible prophage and prophage remnants integrated in the *Streptococcus pyogenes* strain SF370. *Virology*, **302**, 245–258.
15. Haudiquet,M., de Sousa,J.M., Touchon,M. and Rocha,E.P.C. (2022) Selfish, promiscuous and sometimes useful: how mobile genetic elements drive horizontal gene transfer in microbial populations. *Philos. Trans. R. Soc. B Biol. Sci.*, **377**, 20210234.
16. Ibarra-Chávez,R., Hansen,M.F., Pinilla-Redondo,R., Seed,K.D. and Trivedi,U. (2021) Phage satellites and their emerging applications in biotechnology. *FEMS Microbiol. Rev.*, **45**, fuab031.
17. Eppley,J.M., Biller,S.J., Luo,E., Burger,A. and DeLong,E.F. (2022) Marine viral particles reveal an expansive repertoire of phage-parasitizing mobile elements. *Proc. Natl. Acad. Sci. U.S.A.*, **119**, e2212722119.
18. Hackl,T., Laurenceau,R., Ankenbrand,M.J., Bliem,C., Cariani,Z., Thomas,E., Dooley,K.D., Arellano,A.A., Hogle,S.L., Berube,P. *et al.* (2023) Novel integrative elements and genomic plasticity in ocean ecosystems. *Cell*, **186**, 47–62.
19. Angermeyer,A., Hays,S.G., Nguyen,M.H.T., Johura,F., Sultana,M., Alam,M. and Seed,K.D. (2022) Evolutionary sweeps of subviral parasites and their phage host bring unique parasite variants and disappearance of a phage CRISPR-Cas system. *Mbio*, **13**, e03088-21.
20. Perrin,A. and Rocha,E.P.C. (2021) PanACoTA: a modular tool for massive microbial comparative genomics. *NAR Genomics Bioinforma.*, **3**, lqaa106.
21. Ondov,B.D., Treangen,T.J., Melsted,P., Mallonee,A.B., Bergman,N.H., Koren,S. and Phillippy,A.M. (2016) Mash: fast genome and metagenome distance estimation using MinHash. *Genome Biol.*, **17**, 132.
22. Abby,S.S., Néron,B., Ménager,H., Touchon,M. and Rocha,E.P.C. (2014) MacSyFinder: a program to mine genomes for molecular systems with an application to CRISPR-Cas systems. *PLoS One*, **9**, e110726.
23. Néron,B., Denise,R., Coluzzi,C., Touchon,M., Rocha,E.P.C. and Abby,S.S. (2022) MacSyFinder v2: improved modelling and search engine to identify molecular systems in genomes. bioRxiv doi: https://doi.org/10.1101/2022.09.02.506364, 04 September 2022, preprint: not peer reviewed.
24. Steinegger,M. and Söding,J. (2017) MMseqs2 enables sensitive protein sequence searching for the analysis of massive data sets. *Nat. Biotechnol.*, **35**, 1026–1028.
25. Huerta-Cepas,J., Szklarczyk,D., Heller,D., Hernández-Plaza,A., Forslund,S.K., Cook,H., Mende,D.R., Letunic,I., Rattei,T., Jensen,L.J. *et al.* (2019) eggNOG 5.0: a hierarchical, functionally and phylogenetically annotated orthology resource based on 5090 organisms and 2502 viruses. *Nucleic Acids Res.*, **47**, D309–D314.
26. Sievers,F., Wilm,A., Dineen,D., Gibson,T.J., Karplus,K., Li,W., Lopez,R., McWilliam,H., Remmert,M., Söding,J. *et al.* (2011) Fast, scalable generation of high-quality protein multiple sequence alignments using Clustal Omega. *Mol. Syst. Biol.*, **7**, 539.
27. Eddy,S.R. (2011) Accelerated Profile HMM Searches. *PLoS Comput. Biol.*, **7**, e1002195.
28. Moura de Sousa,J.A., Pfeifer,E., Touchon,M. and Rocha,E.P.C. (2021) Causes and consequences of bacteriophage diversification via genetic exchanges across lifestyles and bacterial taxa. *Mol. Biol. Evol.*, **38**, 2497–2512.
29. Sherwin,W.B., Chao,A., Jost,L. and Smouse,P.E. (2017) Information theory broadens the spectrum of molecular ecology and evolution. *Trends Ecol. Evol.*, **32**, 948–963.
30. Katoh,K. and Standley,D.M. (2013) MAFFT multiple sequence alignment software version 7: improvements in performance and usability. *Mol. Biol. Evol.*, **30**, 772–780.
31. Steenwyk,J.L., Buida,T.J., Li,Y., Shen,X.-X. and Rokas,A. (2020) ClipKIT: a multiple sequence alignment trimming software for accurate phylogenomic inference. *PLoS Biol.*, **18**, e3001007.
32. Nguyen,L.-T., Schmidt,H.A., von Haeseler,A. and Minh,B.Q. (2015) IQ-TREE: a fast and effective stochastic algorithm for estimating maximum-likelihood phylogenies. *Mol. Biol. Evol.*, **32**, 268–274.
33. Letunic,I. and Bork,P. (2021) Interactive Tree Of Life (iTOL) v5: an online tool for phylogenetic tree display and annotation. *Nucleic Acids Res.*, **49**, W293–W296.
34. Whelan,F.J., Rusilowicz,M. and McInerney,J.O. (2020) Coinfinder: detecting significant associations and dissociations in pangenomes. *Microb. Genomics*, **6**, e000338.
35. Price,M.N., Dehal,P.S. and Arkin,A.P. (2010) FastTree 2 – approximately maximum-likelihood trees for large alignments. *PLoS One*, **5**, e9490.
36. Afgan,E., Baker,D., Batut,B., van den Beek,M., Bouvier,D., Čech,M., Chilton,J., Clements,D., Coraor,N., Grüning,B.A. *et al.* (2018) The Galaxy platform for accessible, reproducible and collaborative biomedical analyses: 2018 update. *Nucleic Acids Res.*, **46**, W537–W544.
37. Halling,C. and Calendar,R. (1990) Bacteriophage P2 ogr and P4 delta genes act independently and are essential for P4 multiplication. *J. Bacteriol.*, **172**, 3549–3558.
38. Lindqvist,B.H., Dehò,G. and Calendar,R. (1993) Mechanisms of genome propagation and helper exploitation by satellite phage P4. *Microbiol. Rev.*, **57**, 683–702.
39. Kizziah,J.L., Rodenburg,C.M. and Dokland,T. (2020) Structure of the capsid size-determining scaffold of "satellite" bacteriophage P4. *Viruses*, **12**, 953.
40. Novick,R.P. and Ram,G. (2017) Staphylococcal pathogenicity islands — movers and shakers in the genomic firmament. *Curr. Opin. Microbiol.*, **38**, 197–204.
41. Hendrix,R.W., Smith,M.C.M., Burns,R.N., Ford,M.E. and Hatfull,G.F. (1999) Evolutionary relationships among diverse bacteriophages and prophages: all the world's a phage. *Proc. Natl. Acad. Sci*, **96**, 2192–2197.
42. Bibb,L.A. and Hatfull,G.F. (2002) Integration and excision of the *Mycobacterium tuberculosis* prophage-like element, φRv1: integration and excision of φRv1. *Mol. Microbiol.*, **45**, 1515–1526.
43. Kala,S., Cumby,N., Sadowski,P.D., Hyder,B.Z., Kanelis,V., Davidson,A.R. and Maxwell,K.L. (2014) HNH proteins are a widespread component of phage DNA packaging machines. *Proc. Natl. Acad. Sci*, **111**, 6022–6027.
44. LeGault,K.N., Barth,Z.K., DePaola,P. and Seed,K.D. (2022) A phage parasite deploys a nicking nuclease effector to inhibit viral host replication. *Nucleic Acids Res.*, **50**, 8401–8417.
45. McKitterick,A.C., Hays,S.G., Johura,F.-T., Alam,M. and Seed,K.D. (2019) Viral satellites exploit phage proteins to escape degradation of the bacterial host chromosome. *Cell Host Microbe*, **26**, 504–514.
46. de Laat,W.L., Jaspers,N.G.J. and Hoeijmakers,J.H.J. (1999) Molecular mechanism of nucleotide excision repair. *Genes Dev.*, **13**, 768–785.
47. Tommasini,D., Mageeney,C.M. and Williams,K.P. (2022) An integrase clade that repeatedly targets prophage late genes, yielding helper-embedded satellites. bioRxiv doi: https://doi.org/10.1101/2022.07.18.500453, 19 July 2022, preprint: not peer reviewed.
48. Boyd,C.M., Angermeyer,A., Hays,S.G., Barth,Z.K., Patel,K.M. and Seed,K.D. (2021) Bacteriophage ICP1: a persistent predator of *Vibrio cholerae*. *Annu. Rev. Virol.*, **8**, 285–304.
49. Haag,A.F., Podkowik,M., Ibarra-Chávez,R., Gallego del Sol,F., Ram,G., Chen,J., Marina,A., Novick,R.P. and Penadés,J.R. (2021) A regulatory cascade controls Staphylococcus aureus pathogenicity island activation. *Nat. Microbiol.*, **6**, 1300–1308.
50. Touchon,M., Bernheim,A. and Rocha,E.P. (2016) Genetic and life-history traits associated with the distribution of prophages in bacteria. *ISME J.*, **10**, 2744–2754.